

3.2 The Eckert and Diaguila Mixed Convection Heat Transfer Tests⁽⁶⁾

(to assure a constant velocity)

Eckert and Diaguila⁽⁶⁾ conducted heat transfer tests on a vertical tube that was 13.5-feet high with a 23.25-inch inside diameter. Inlet and outlet air pipes and dense screens were located at each end. A 10-foot steam jacket supplied steam slightly superheated as the heat source. Sixteen condensation chambers collected and piped condensate to a station where the flow rate was measured and the local heat flux was determined. An air flow at approximately 80°F, at pressures from 1 atmosphere to 99 psia, was forced through the test section. Tests were conducted with forced flow in both the upward (assisting mixed convection) and downward (opposed mixed convection) direction.

Thermocouples at the tube center and in the tube wall provided a temperature difference from which the local heat transfer coefficient could be determined. The test data were used to validate the mixed convection heat transfer correlation at prototypic Reynolds and Grashof numbers.

The Nusselt number, Nu , is defined as $Nu = hd_h/k$, where d_h is the hydraulic diameter. Entrance-effect multipliers were calculated as described in Section 2.2 and are presented in Table 3.2-1. The mixed convection Nusselt numbers were calculated as described in Section 2.1. The calculated Nusselt number for each of the ten assisting convection tests are compared with the measured data, and are shown as a function of the dimensionless height in Figures 3.2-1 through 3.2-10. The relevant test parameters are presented in Table 3.2-2.

**TABLE 3.2-1
ENTRANCE-EFFECT MULTIPLIERS FOR THE ECKERT AND
DIAGUILA HEAT TRANSFER TESTS**

	Distance from bottom, ft															
	0.63	1.25	1.88	2.50	3.13	3.75	4.38	5.00	5.63	6.25	6.88	7.50	8.13	8.75	9.38	10.0
Multiplier for $d_h = 1.94$ ft.	2.89	1.44	1.30	1.24	1.20	1.17	1.15	1.14	1.13	1.12	1.11	1.10	1.10	1.09	1.09	1.08

9809300043 980922
PDR ADOCK 05200003
A PDR

Enclosure 1

As discussed in the reference report, heat flux to the plate was determined experimentally using heat flux meters and by performing coolant energy balances, resulting in an uncertainty within ± 3 percent associated with the reported heat flux measurements.

Chromel-constantan (Type E) thermocouples were used for all test temperature measurements. Assuming a typical Type E thermocouple accuracy of $\pm 0.5^\circ\text{C}$ and an instrumentation error of $\pm 0.02^\circ\text{C}$ results in a total uncertainty of $\pm 0.5^\circ\text{C}$ or $\pm 0.9^\circ\text{F}$.

Duct air velocity measurements in the Wisconsin Condensation Tests⁽²³⁾ were obtained using a pitot tube and pressure transducer as in the Westinghouse Flat Plate Tests⁽²⁰⁾. Assuming instrumentation similar to that considered in Subsection 4.5.1 was used in the Wisconsin Condensation Tests and that the resulting air velocity measurement uncertainty of 0.32 ft./sec is typical for the range of recorded test velocities results in an air velocity measurement uncertainty of 0.32 ft./sec or 0.098 m/sec.

These test measurement uncertainties result in measured Sherwood number uncertainty within ± 12 percent for the reported University of Wisconsin condensation tests⁽²³⁾.

4.4.4 Open Literature Tests

Information on

^ Uncertainties in the Hugot⁽¹¹⁾, Eckert and Diaguila⁽⁶⁾, Siegel and Norris⁽¹⁹⁾, Gilliland and Sherwood⁽²²⁾, and Chun and Seban⁽⁷⁾ tests ~~are discussed in the~~ open literature references.

^ is limited to what is provided in these

The AP600 riser channel differs from the test geometries due to the 6-foot well, or turning region at the bottom of the baffle. For modeling simplicity it is desirable to use a fully-developed heat transfer coefficient over the full channel height. The following subsections show the use of a fully-developed heat transfer coefficient over the full riser height is conservative. The calculations show the heat transfer decrease (relative to fully-developed heat transfer) is more than offset by the heat transfer increase due to neglecting the entrance effect in the channel above the well. The geometric features of the well region and riser channel are shown in Figure 2.1-4.

2.2.1 Heat Transfer in the Well Region Below the Baffle

The annular duct created by the baffle for the AP600 starts 6 feet above the bottom of an annular "well." This well is ^{4.5}8 feet wide and is heated on the inside surface. In the AP600 evaluation model it is assumed, for simplicity, that the forced convection heat transfer correlations used in the annular region can be applied within this region as well. It is more realistic to assume a free convection heat transfer relationship on the heated containment shell side of the well.

Although the upper half of the 6-foot height may undergo transition to turbulent free convection, the laminar free convection correlation predicts lower heat transfer coefficients and is used. The effect of using forced convection in the 6-foot well is evaluated by comparing the total heat transfer calculated with laminar-free convection in the well to the total heat transfer calculated with forced convection everywhere.

The empirical formula of McAdams⁽³⁾ was chosen for the laminar free convection mean Nusselt number:

$$\overline{Nu} = 0.555(Ra_x)^{1/4} \quad (8)$$

The Nusselt number for forced flow convection is given by the Colburn⁽⁴⁾ relationship:

$$Nu = 0.023Re^{4/5}Pr^{1/3} \quad (9)$$

Assuming the active length of the annulus above the baffle is 90 feet, then the active heat transfer length is 96 feet. The fractional decrease in total heat transfer over the 96-foot height due to free convection in the 6-foot well region is equal to the factor ϕ determined by length-weighting. Equations (8) and (9):

$$\phi = \frac{6}{96} \left(1 - \frac{2(.555)}{6(.023)} \frac{Ra_x^{1/4}}{Re^{4/5}Pr^{1/3}} \right) \quad (10)$$

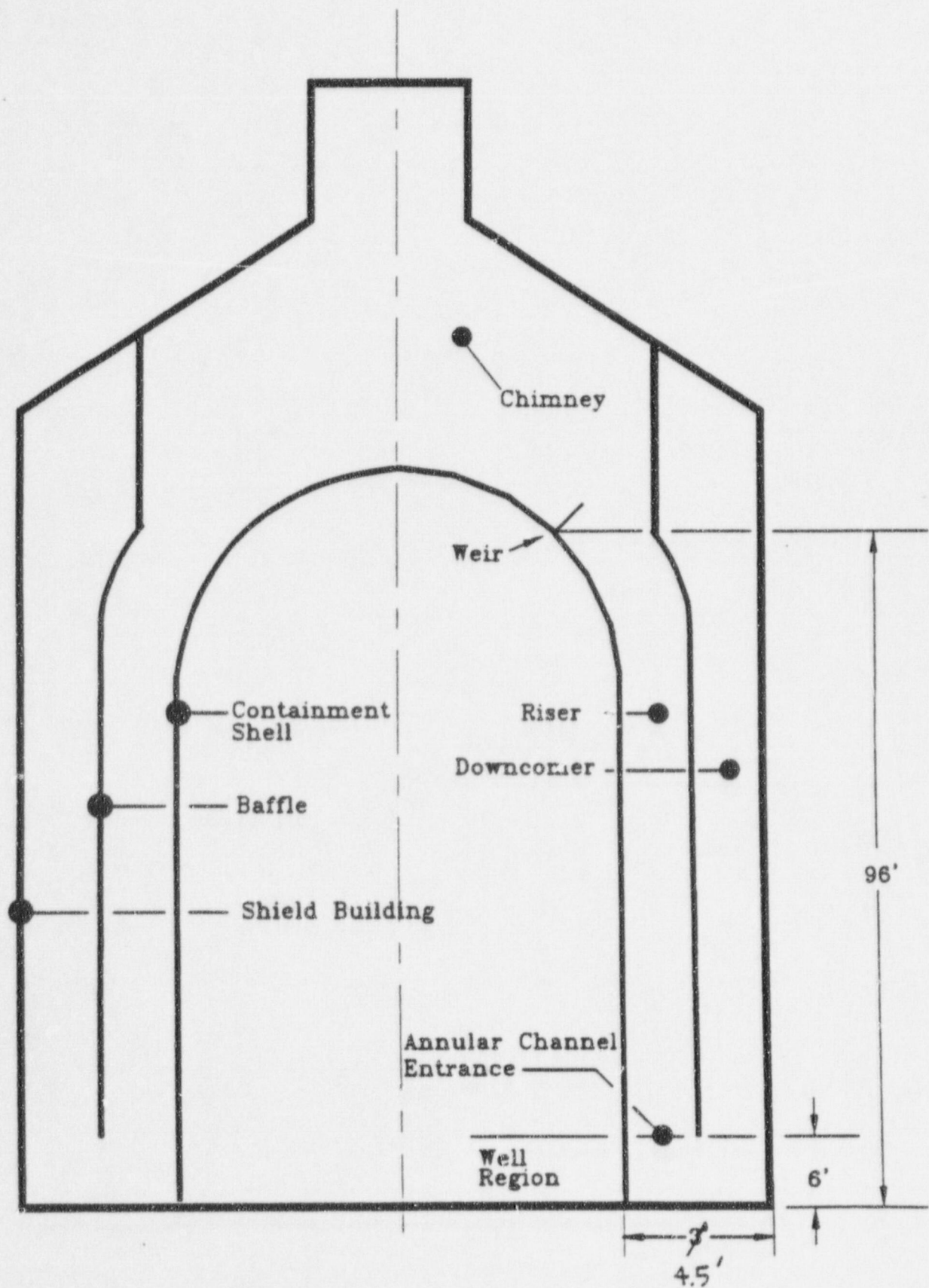


Figure 2.1-4 PCS Air Flow Path Features

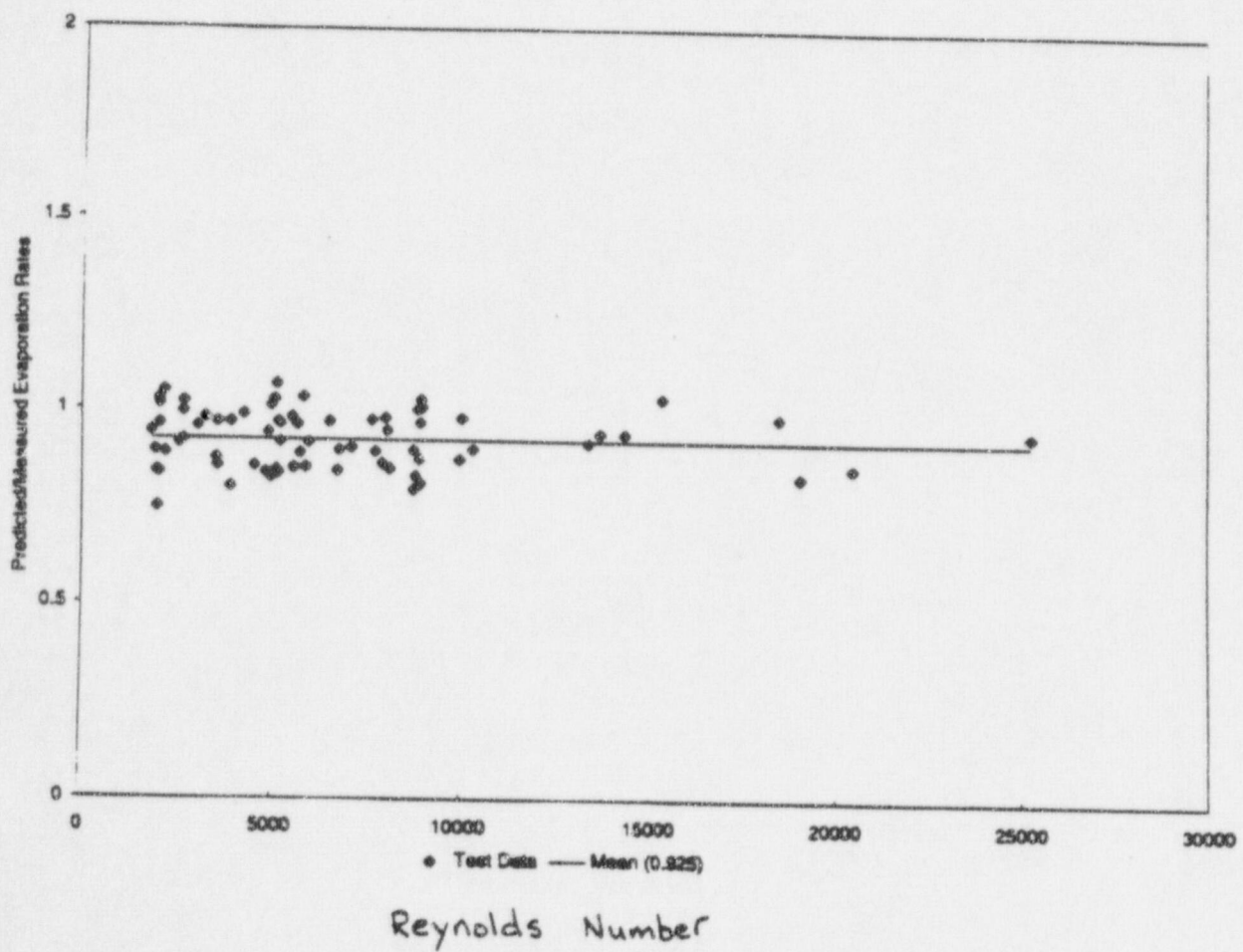


Figure 3.6-2 Comparison of Predicted-to-Measured Evaporation Rates for the Gilliland and Sherwood Evaporation Tests

- [REDACTED]
14. Eckert, E. R. G., Drake Jr., R. R., *Analysis of Heat and Mass Transfer*, 1972, McGraw-Hill.
 15. Kestin, J., et al., *J. Phys. Chem. Ref. Data*, 13, 229, 1984.
 16. Rohsenow, W. M., Hartnett, J. P., *Handbook of Heat Transfer*, 1973, McGraw-Hill.
 17. Bird, R. B., Stewart, W. E., Lightfoot, E. N., *Transport Phenomena*, 1960, John Wiley & Sons.
 18. "WGOthic Application to AP600," WCAP-14407, Section 3, September 1996, Westinghouse Electric Corporation.
 19. Siegel, R., Norris, R. H., "Test of Free Convection in a Partially Enclosed Space Between Two Heated Vertical Plates," *Journal of Heat Transfer*, April 1957.
 20. Stewater, W. A., Pieczynski, A. T., Conway, L. E., "Tests of Heat Transfer and Water Film Evaporation on a Heated Plate Simulating Cooling of the AP600 Reactor Containment," WCAP-12665, April 1992, Westinghouse Electric Corporation.
 21. "Heavy Water Reactor Facility (HWRF) Large-Scale Passive Containment Cooling System Confirmatory Test Data Report," HWRF-RPT-93-001, July 1993.
 22. Gilliland, E. R., Sherwood, T. K., "Diffusion of Vapors into Air Streams," *Industrial and Engineering Chemistry*, Vol. 26, No. 5, pp. 516-523.
 23. Huhtiniemi, L., Pernsteiner, A., Corradini, M. L., (University of Wisconsin), "Condensation in the Presence of a Noncondensable Gas: Experimental Investigation," WCAP-13307, April 1991, Westinghouse Electric Corporation.
 24. Peters, F. E., "Final Data Report for PCS Large-Scale Tests, Phase 2 and Phase 3," WCAP-14135, ~~July 1994~~, Westinghouse Electric Corporation.
^
Rev. 1, April 1997,

4.5 Mass Transfer Correlation Biases

The mass transfer correlations selected for use on AP600 were compared to data from both SETs and integral effects tests (IETs). The data comparisons were presented in the form of predicted-to-measured Sherwood numbers. The comparisons show the correlations underpredict the data with mean predicted-to-measured values of 0.936 for evaporation and 0.988 for condensation. Thus, the selected correlations exhibit an underprediction of the mean data.

As a conservative approach the correlations can be biased, ~~such that the data points that are most overpredicted with the nominal correlation are bounded, and the remainder of the data set is underpredicted. That is, the biased correlation bounds all the data.~~ This can be expressed as: *

$$C \frac{P}{M} \leq 1 \quad (21)$$

where:

- C is the bias factor
- P is the predicted mass transfer coefficient value
- M is the measured mass transfer value

Thus, the value for C can be determined from the most overpredicted data point as:

$$C \leq \frac{M}{P} \quad (22)$$

The evaporation test data are plotted in Figure 4.2-3 and have a peak value of $P/M = 1.191$. Thus, the value of the bias factor for the evaporating data is $C = 0.840$. ~~By multiplying the evaporation mass transfer correlation by this factor, the correlation conservatively bounds the test data. The predicted-to-measured Sherwood number calculated with the bounding correlation is shown in Figure 4.2-3.~~ ~~conservatively biased.~~ *

The condensation test data are plotted in Figure 4.3-3 and have a peak value of $P/M = 1.541$. This particular value lies somewhat above the bulk of the data and corresponds to a single elevation on the LST, while five other simultaneous measurements at different elevations in the same test produced lower P/M values. This peak value is considered a local anomaly that does not represent integral condensation rates. Consequently, the next highest value, $P/M = 1.369$ was selected for evaluating the bias factor. Thus, the value of the bias factor for the ^{condensing} evaporating data is $C = 0.730$. ~~By multiplying the condensation mass transfer correlation by this factor, the correlation conservatively bounds the test data. The predicted-to-measured Sherwood number calculated with the bounding correlations is shown in Figure 4.3-3.~~ ~~conservatively biased.~~ *

ATTACHMENT 2

Markups to WCAP-14845 Rev 2, "Scaling Analysis for AP600 Containment Pressure During Design Basis Accidents"

(Page E-5): The data table, which supports statement on validation of equation, is no longer part of the report. Was Table 10-8, Section 10.2.1.1.

RESPONSE:

The second bullet on pg. E-5 refers to the mean deviation of less than 0.01 and the standard deviation of 0.13 which were provided in Table 10-8 of WCAP-14845, Rev. 0. This table was deleted from the revised scaling report because the information in the table was not needed to support the results of the top-down system level scaling described in Part III of the revised report. The second bullet on page E-5 is an accurate statement that is supported by a Westinghouse calculation note. Descriptive text and the information from Table 10-8 (from WCAP-14845, Rev. 0) will be added as a new appendix. Reference to this new appendix will be added to the second bullet on page E-5.

(Page E-8): The is no Figure 11-1. Is it 10 5?

RESPONSE:

Figure 11-1 should be Figure 10-5. The Scaling Analysis document will be revised to change the references to Figure 11-1 on pages E-8 and 12-3 to Figure 10-5.

(Page E-8): Last paragraph. Where and what is the support, code version(1.x,4.x), models (LP,DP, errors), etc.? In what section (sections) can this material be found?

RESPONSE:

WCAP-14845 will be revised to define the Evaluation Model by reference to WCAP-14407, Rev 1, Section 4.

(Page P-2): Thought GOTHIC was selected but needed additional model for the clime. WGOTHIC was result of effort.

RESPONSE:

The sentence in question will be revised to state that GOTHIC was selected as the best available tool. The third paragraph under "Element 1" will also be revised.

(Page P-4): LST ref. is old June 1994 report. April 1997 revisions indicates potential for bad analyses if based on original.

RESPONSE:

The test data used in the Scaling Analysis are all consistent with the April 1997 issue of WCAP-14135, Rev. 1. Reference 10 on page 14-1 will be corrected.

(Page P-6): Distributed parameter model? Role and status. Is there a summary or which sections describe use of this model?

RESPONSE:

The reference to the distributed parameter model will be removed from WCAP-14845, page P-6.

(Page 1-5): Ref. to Ref. 4? Should be Ref. 5. Section 9 of 4 is not to be reviewed.

RESPONSE:

Yes, Reference 4 should be Reference 5. WCAP-14845 will be revised to refer to Reference 5.

(Page 2-1): What is the mixing and stratification report? Section 9 of WCAP-14407?

RESPONSE:

Yes. WCAP-14845 will be revised to change "mixing and stratification report" to Reference 5, Section 9.

(Page 8-3): There is no shading visible on Table 8-3, or any other table (8-4 and 8-5), to indicate > 10%.

RESPONSE:

WCAP-14845 will be revised to correct the discrepancy. The shading will be added to the tables.

(Page 10-5): 2%, is it non-conservative?

RESPONSE:

WCAP-14845 will be revised to note that the Colburn correlation used for AP600 predicts 2% higher heat transfer coefficients than does Dittus-Boelter, or Seider-Tate. The Colburn correlation differs little, but is 2% less conservative than the alternatives.

(Page 11-6): There is no Table 10-10. Table 10-3?

RESPONSE:

Yes, WCAP-14845 will be revised to change Table 10-10 (2 places) to Table 10-3.

Westinghouse has prepared AP600 Response to Requests for Additional Information as an enclosure to letter NSD-NRC-97-5216 of June 27, 1997. The majority of the responses appear to be acceptable. However, comments and clarifications apply to the following RAIs:

- (1.) (RAI 480.975) Pi-groups $pi_{p,g,j}$ and $pi_{e,f,jf}$ have not been replaced in Table 2-1 as stated in the response. Please clarify where numerical values for these pi-groups can be found.

RESPONSE:

The subscript "p,g,j" should be p,q,j, which indicates a pressure pi group, p, for sensible (radiation plus convection) heat transfer, q, from heat sink j. j is an index that represents the heat sinks listed in Table 7-1. Values of $pi_{p,q,j}$ are presented for each time phase in Table 8-5. WCAP-14845 will be revised to correct this subscript error in Table 2-1.

WCAP-14845 will be revised to replace the group $pe_{e,f,jf}$ by $pe_{e,f,j}$ and $pe_{e,q,ssx}$ to be consistent with Note 1 to Table 2-1.

- (2.) (RAI 480.995) In the previous revision of the scaling report, the Biot number had been calculated to be 0.08. Now it has been recalculated as 0.13. According to Kreith, Principles of Heat Transfer, 3rd ed., p. 140, a criterion for treating a heat structure as a lumped mass is that the Biot number be less than 0.1. Since Kreith's criteria is no longer satisfied, what is the justification for lumping the steel? What is the estimated magnitude of the error introduced by this approximation?

RESPONSE:

Kreith's Biot criteria $Bi < 0.1$, is based on a temperature error of less than 5%. It is estimated that $Bi < 0.13$ would give a temperature error of less than 10%. Such an error is considered acceptable for a scaling analysis in view of the simplicity of the lumped parameter assumption.

Westinghouse will review the use of Biot number and the discussion provided in the Heat & Mass Transfer Report, the PIRT, and the Application Report. Text will be updated as needed for consistency and clarification.

- (3.) (RAI 480.1002) There still appears to be a problem with the nomenclature in equation 135 and in the equation on the second line of page 7-30. Why is it necessary to change the temperature subscripts in going between these two equations? Also, the subscript "scx" (not in the nomenclature section or in Figure 7-3) is not defined.

RESPONSE:

WCAP-14845 will be revised to replace the undefined subscripts sc and scx with the defined subscripts ss and ssx. That will correct the inconsistency in Equation 135 and the equation on the second line.

- (4.) (RAI 480.1011) The stated revision to the text does not appear to have been made.

RESPONSE:

WCAP-14845 will be revised to state that the riser and downcomer both operate in forced convection, consistent with Figure 4-1.

- (5.) (RAI 480.1017) The RAI was directed toward determining whether any of the remaining pi-group values contained an anomaly similar to that for $pi_{c,bf}$. The NRC review did not check the value of every pi-group. Please provide an evaluation of the anomaly effect for $pi_{ic,dSX}$ and $pi_{c,esx}$.

RESPONSE:

Although the pi value may appear anomalous, the temperature and heat transfer rate calculations are correct. The individual heat transfer coefficients and the corresponding temperature differences for the baffle inside, the dry shell outside, and the evaporating shell outside are presented in Table 1. The values show the convection and radiation heat transfer coefficients range from 1.5 to 2.7, a reasonable range. When multiplied by the corresponding DT the heat transfer rate is also reasonable. However, when the small negative riser-to-baffle temperature difference is used to normalize the baffle heat transfer rate the anomaly appears. The anomaly only appears in the baffle equation since the evaporating and dry shell DT's are all relatively large values.

The selection of a different normalizing temperature difference would change the apparent anomaly for the baffle, but would not change the resulting temperatures and heat fluxes. Or, as stated in RAI 480.1017, expressing the energy equation in terms of the riser-baffle and shell-baffle temperature differences instead of only the riser-baffle temperature difference would also eliminate the anomaly.

Table 1 - Temperature Differences and Heat Transfer Coefficients for the Shell and Baffle

	Evaporating Shell	Dry Shell	Baffle
Evaporation Energy Transfer	$h_{m,esx} = 126.6$		$h_{m,ri-bf} = 0$
	$DT_{xf-ri} = 41.62$		$DT_{ri-bf} = -0.04$
Convection Heat Transfer	$h_{c,esx} = 2.73$	$h_{c,dSX} = 2.67$	$h_{c,ri-bf} = 2.47$
	$DT_{xf-ri} = 41.62$	$DT_{dSX-ri} = 113.21$	$DT_{ri-bf} = -0.04$
Radiation Heat Transfer	$h_{r,esx} = 1.50$	$h_{r,dSX} = 1.78$	$h_{r,shx-bf} = 1.60$
	$DT_{xf-bf} = 41.58$	$DT_{xf-bf} = 113.17$	$DT_{shx-bf} = 41.59$
Liquid Film Heat Transfer	$h_{xf} = 840$		
	$DT_{xf-bf} = 6.49$		

6. (RAI 480.1026) Why does increasing heat transfer coefficient with increasing Reynolds Number imply that there is no concern?

RESPONSE:

Our understanding of the concerns expressed in the RAI are that the test data range does not cover the AP600 range, and that the heat transfer coefficient may misbehave at higher Reynolds numbers. The Chun and Seban data cover Reynolds numbers up to 20,000, or approximately 5 times higher than the highest AP600 Reynolds number, so it is clear the data cover the AP600 range. The test data show the Nusselt number and heat transfer coefficient continue to increase uniformly as the Reynolds number increases, and that the correlation models the data. Consequently it is highly unlikely that the minimum heat transfer coefficient value has been missed.

- (7.) (RAI 480.1027) In addition to the information in the RAI, the following is needed to complete the review. Please compare the physical film thickness (as predicted by the Nusselt equation) to the Chun and Seban effective film thickness over the range of Reynolds Numbers expected for AP600 (both inside and outside the PCS, above and below the second weir). For each Reynolds number, compare the heat transfer coefficient for the water film using the Nusselt model to the Chun and Seban model.

The wording in the first paragraph of Section 7.4 has been improved to distinguish the effective film thickness from the physical film thickness. Unfortunately, in the second paragraph, the effective film thickness is used to get the heat capacity of the film, whereas the physical thickness should be used. The difference in the ratio calculated is not significant, but it confuses the issue, in the sense that it encourages the reader to think of the effective thickness as a physical distance.

RESPONSE:

The Nusselt equation models the smooth laminar film flow that exists for film Reynolds numbers less than 30. Consequently it is not appropriate to apply the Nusselt correlation to wavy laminar and turbulent film flows. The result of misapplying the Nusselt smooth laminar film correlation to higher Reynolds numbers is to predict a thicker film with lower heat transfer coefficient than given by the Chun and Seban correlation.

Since the heat capacity of the liquid film depends on the mass of liquid, a measure of the average film thickness is needed to estimate the volume and resulting mass. The effective thickness, determined from the film heat transfer coefficient correlation, is a reasonable measure of the average thickness. In light of the small value of the estimated heat capacity, and the transient energy storage, a more rigorous measure of the average film thickness is not required.

Westinghouse will add Kutataladze data to Figure 10-3 of the Scaling Report to provide further basis for the nominal Chun and Seban correlation. In addition, further justification in the text will be provided. This will include a discussion of the distinction between physical and effective film thickness. Westinghouse will also perform a sensitivity calculation varying film thickness to confirm the Low ranking of this phenomenon.

- (8.) (RAI 480.1031) In Table 10-3 the new footnote reveals that for LST, measured air/steam concentrations were used since LST is not homogeneous. How were air steam concentrations for AP-600 determined for use in calculating the pi-group values?

RESPONSE:

The AP600 air/steam concentrations were determined from the Scaling Model, that assumes the total mass of gas is well mixed. Westinghouse will add a reference to Appendix 9.C of the WGOTHIC Application Report and also include a summary of the hand calculation results related to stratification gradient.

9. (RAI 480.1032) The definition of distortion provided appears to be appropriate for phenomena which are quantified by pi-groups. However, some phenomena, such as mixing and stratification are not represented by pi-groups. A broader definition of distortion appears to be needed to cover phenomenon not quantified by pi-groups.

RESPONSE:

Westinghouse has used conventions and definitions from the literature as guidance for the containment pressure scaling analysis. The literature typically defines distortion in terms of pi groups, so there is no known convention for defining distortion for groups that appear as parameters in pi groups, rather than as pi groups.

- (10.) (RAI 480.1035) Reference to the WGOTHIC Application Report, Appendix 7.A, which you state was added could not be found. The reference citation should appear in the section titled "External Water Flow Time Variations" on page 11-7.

RESPONSE:

WCAP-14845 will be revised to include a reference to WCAP-14407, Rev. 1, Section 7.6.3, that includes the maximum and minimum film flow rate values, and the uses for the values. (Since RAI 480.1035 was written, WCAP-14407 was revised.)

11. (RAI 480.1036) The conclusions still appear to be somewhat disjoint from the main body of the report. For example, the discussion in item 1 would seem to be supported more by the Applications Report than this Scaling Report.

RESPONSE:

The discussion in Conclusion item 1 identifies the high and medium ranked phenomena that were confirmed by the scaling analysis. The conclusions also provide information from WCAP-14326 and WCAP-14407 that tells how the phenomena are conservatively modeled. Westinghouse will add summary statements for each of the referenced sections.

Top-Down System-Level Scaling

- The comparison shows the scaled LST captures the high ranked phenomena associated with the AP600 containment pressurization during blowdown. However, internal field characteristics during and after blowdown cannot be predicted with the lumped parameter evaluation model.
- Nominal predictions of the steady-state scaling equations using free convection heat and mass transfer inside containment and measured air/steam concentrations for 21 steady-state LST cases show the average steady-state mass and energy transfer rates are predicted with a mean deviation of less than 0.01 and a standard deviation of 0.13. (Appendix A) Such agreement is considered to verify that the mass and energy equations accurately predict the transfer rates, thereby validating the mass and energy scaling equations. The transient RPC equation is the result of combining the mass and energy rate equations with the equation of state. At steady-state conditions, the terms on the right-hand side of the RPC equation represent the equivalent mass and energy rate terms. Therefore, validation of the steady-state scaling equations implicitly validates the RPC equation. *
- The detailed breakdown of individual pi groups shows that during all the phases of a DECLG LOCA, phenomena associated with the drops, pools, chimney, and baffle are not important and can therefore be neglected since the pi group numerical values are of order less than 0.1. The only pi groups of any significance are those associated with the solid internal heat sinks and the shell. These internal heat sinks become saturated prior to the time when quasi-steady operation occurs. Therefore, only the pi groups identified as containment or shell are calculated for the AP600 plant and LST at steady-state. The LST was scaled to AP600 at a steady-state corresponding to conditions in AP600 expected at 4000 to 5000 seconds into the transient. The scaling comparison shows the dominant terms are the source, condensation, and evaporation, all of which scale to within 8 percent.

Differences and Distortions between the LST and AP600

- The LST heat sink area/volume ratios and flow history do not scale to AP600 and thus prevent the use of the LST as a transient IET representation of AP600. However, those distortions do not prevent the use of the LST results to validate the high-ranked, separate effects phenomena of condensation mass transfer and liquid film stability and coverage. The temperature and concentration measurements from the LST provide some of the data needed to understand and bound stratification in the AP600 evaluation model. Heat transfer measurements from tests with no external water provided data to validate dry heat transfer to the riser. In addition, the steady-state LST results are used to validate separate effects aspects of the evaluation model.

APPENDIX A

Validation of Steady-State Mass and Energy Transfer Equations

The constitutive equations for steady-state heat and mass transfer inside and outside the LST were coupled and solved using properties measured on the LST as boundary conditions. The containment total pressure, steam pressure, and bulk temperature defined the state inside the LST. The riser gas velocity, bulk riser gas temperature, wetted fraction, and the external water flow rate and temperature define the state outside the vessel. The heat and mass transfer rates inside and outside were calculated for the subcooled, evaporating and dry regions.

The measured values for $\dot{m}_{g,brk,o}$ and $\dot{m}_{g,brk,o}\Delta h_{g,brk,o}$ were used to normalize the predicted values, respectively, for mass and for energy that define the pi values in Equations (199). The results are summarized in Table A-1 for 21 LST cases. All tests are included that had measured steam concentrations and the steam source located under the steam generator model. The results show the average quasi steady-state mass and energy transfer rates are very close to zero, with a standard deviation of 0.13. Such agreement is considered good for such a simple model. These results verify that the mass and energy equations used in the scaling analysis accurately predict the transfer rates, thereby validating the equations.

Table A-1 Energy Rate of Change Equation Comparison to Steady-State LST					
Large-Scale Test	Pressure psia	Temperature °F	$\dot{m}_{g,brk,o} \Delta h_{g,brk,o}$ BTU/sec	$1 - \frac{\sum(\pi_{e,fg,j} + \pi_{e,fl,j} + \pi_{e,q,j})}{\pi_{m,j}}$	$1 - \sum \pi_{m,j}$
212.1A	23.77	334.3	427.2	-0.167	-0.197
212.1B	29.36	317.8	667.8	-0.058	-0.076
212.1C	36.93	317.7	963.4	-0.036	-0.948
213.1A	23.5	334.3	398.2	-0.185	-0.213
213.1B	28.83	327.0	642.1	0.039	0.022
213.1C	40.29	319.6	980.6	0.324	0.321
216.1A	32.44	326.5	706.7	-0.173	-0.206
216.1B	50.18	329.1	711.7	0.092	0.068
217.1A	42.37	314.9	1320.7	0.142	0.141
217.1B	50.86	319.7	1303.9	0.116	0.115
218.1A	42.44	314.0	1329.4	0.051	0.047
218.1B	50.05	317.6	1250.3	-0.001	-0.001
219.1A	34.97	343.0	145.9	0.082	0.088
219.1B	41.89	343.8	148.1	0.086	0.102
219.1C	23.24	340.2	143.8	-0.001	0.016
221.1A	19.36	339.6	185.7	-0.117	-0.132
221.1B	26.02	333.2	189.5	0.089	0.080
221.1C	63.36	336.7	186.0	0.098	0.106
222.1	99.66	331.1	719.1	-0.158	-0.167
224.1	45.51	298.9	309.5	-0.118	-0.064
224.2	55.54	310.4	712.2	-0.106	-0.087
Average =				-0.00001	-0.004
Standard Deviation				0.128	0.133

The scaling analysis shows the three primary drivers, or dominant system level phenomena, for the pressure transient are the break source, the gas volume, and the heat sink surface area dependent condensation rate. The scaling analysis shows the system response is well scaled (properly weights dimensionless groups for these three dominant phenomena as shown in Figure 11-1) for small values of dimensionless time and for longer values of dimensionless time, and shows a distortion for intermediate times. The magnitude of the distortion in the mid-range is too large to claim the LST pressure transient directly scales to AP600 in this range. However, the distortion is small enough that the LST data can be used to examine known lumped parameter modeling biases in the bounding evaluation model.

Furthermore, testing the evaluation model against a range of LST cases, with step changes in boundary conditions (source flow rate, external fan, external water on or off) is expected to cover the range of system level dimensionless groups for AP600 operation through the refill and peak pressure time phases between the blowdown and quasi-steady long term operation. This coverage is expected because the boundary condition variations result in a range of relative values of condensation rate and steam pressure.

described in Reference 5, Section 9,

The lumped parameter Evaluation Model does not resolve internal velocity and concentration fields due to its simplified momentum model and large lumped volumes. Comparisons between early versions of the evaluation model and the system level LST response showed that pressure was reasonably well predicted, with a modest conservative margin. Examination of internal processes clearly identified the existence of competing internal effects in which the excessive velocities predicted by the lumped parameter model overpredicted the velocity component of mass transfer, while overmixing underpredicted the steam concentration component of mass transfer. Consequently, it is required to address competing effects in AP600 predictions. The effect of overpredicted velocities was easily resolved by using only free convection for internal heat and mass transfer, thereby eliminating velocity from the condensation correlation. The overmixing issue was resolved by carefully examining and biasing the effects of circulation and stratification in the evaluation model as discussed in Reference 5, Section 9.

The scaling analysis shows the three primary drivers, or dominant system level phenomena, for the pressure transient are the break source, the gas volume, and the heat sink surface area dependent condensation rate. The scaling analysis shows the system response is well scaled (properly weights dimensionless groups for these three dominant phenomena as shown in Figure 11-1) for small values of dimensionless time and for longer values of dimensionless time, and shows a distortion for intermediate times. The magnitude of the distortion in the mid-range is too large to claim the LST pressure transient directly scales to AP600 in this range. However, the distortion is small enough that the LST data can be used to examine known lumped parameter modeling biases in the bounding evaluation model. *

Furthermore, testing the evaluation model against a range of LST cases, with step changes in boundary conditions (source flow rate, external fan, external water on or off) is expected to cover the range of system level dimensionless groups for AP600 operation through the refill and peak pressure time phases between the blowdown and quasi-steady long term operation. This coverage is expected because the boundary condition variations result in a range of relative values of condensation rate and steam pressure.

The lumped parameter Evaluation Model does not resolve internal velocity and concentration fields due to its simplified momentum model and large lumped volumes. Comparisons between early versions of the evaluation model and the system level LST response showed that pressure was reasonably well predicted, with a modest conservative margin. Examination of internal processes clearly identified the existence of competing internal effects in which the excessive velocities predicted by the lumped parameter model overpredicted the velocity component of mass transfer, while overmixing underpredicted the steam concentration component of mass transfer. Consequently, it is required to address competing effects in AP600 predictions. The effect of overpredicted velocities was easily resolved by using only free convection for internal heat and mass transfer, thereby eliminating velocity from the condensation correlation. The overmixing issue was resolved by carefully examining and biasing the effects of circulation and stratification in the evaluation model as discussed in Reference 5, Section 9.

Review by representatives of industry, academia, and regulatory agencies were incorporated into the process. The end result is documentation that describes the PCS DBA evaluation model and its bases in an auditable, traceable manner. Following is a brief description of the four major process elements.

Element 1 Determine AP600 PCS Modelling Requirements

The PCS DBA methodology development process began with a review of the AP600 design and DBA scenarios and an identification of phenomena important for AP600 containment pressurization. This review identified several separate effects tests (SETs) to investigate specific phenomena such as the liquid flow over the outside of the containment shell, and condensation and evaporation mass transfer. In addition, integral effects tests (IETs) at two different scales were also identified to examine the integrated heat and mass transfer behavior of the PCS. The need for such tests was recognized and testing was initiated in the late 1980's. Table P-1 was used to identify the containment phenomena unique to AP600 and the tests required to validate models of those phenomena. From this review, the ~~Westinghouse-GOTHIC (WGOTHIC)~~ computer code was selected as the best available tool to evaluate containment pressure.

A phenomena identification and ranking table (PIRT) is developed to identify the key thermal-hydraulic phenomena which govern the transients of interest. To allow definition of the relevant phenomena, plant design parameters and design basis scenarios are first defined. The PIRT (Reference 3) then ranks phenomena according to their relative importance to the particular transient phase of interest. The PIRT process included input and review by representatives of industry, academia, cross-functional Westinghouse technical reviews, and regulatory authorities. The bases for high, medium, and low rankings are documented in Reference 3 which also documents evaluation model requirements and approaches to address and bound important phenomena. A key result of the PIRT is that the dominant phenomenon for transferring energy from the containment is mass transfer - condensation on the inside and evaporation on the outside. Phenomena ranked high or medium during any accident phase are investigated, and methods to bound uncertainties are developed (see Element 3 below). Phenomena with a low ranking do not significantly influence the containment pressure response; thus, models that capture the gross behavior are sufficient, and where justifiable, a low ranked phenomenon may be neglected entirely. Section 2 summarizes the PIRT high and medium ranked phenomena and the approach that is used to address each.

The ~~WGOTHIC~~ computer code was ~~selected~~, upgraded, and ~~frozen~~ to allow explicit modeling of many of the phenomena identified in the initial review. As the scaling analysis and testing programs progressed, code upgrades to better model experimental results were completed according to guidelines consistent with life-cycle management identified in

As a result, the Westinghouse-GOTHIC (WGOTHIC) code was created.

14 REFERENCES

1. NSD-NRC-97-4968, *AP600 Passive Containment Cooling System Design Basis Analysis Reports*, January 31, 1997.
2. "AP600 Standard Safety Analysis Report," June 26, 1992, Westinghouse Electric Corporation.
3. M. J. Loftus, D. R. Spencer, J. Woodcock, "Accident Specification and Phenomena Evaluation for AP600 Passive Containment Cooling System," WCAP-14812, Rev. 1, June 1997, Westinghouse Electric Corporation.
4. D. L. Paulsen, et al., "WGOTHIC Code Description and Validation," WCAP-14382, May 1995, Westinghouse Electric Corporation.
- * 5. ~~D. L. Paulsen, et al.~~, "WGOTHIC Application to AP600," WCAP-14407, Rev 1, ~~June~~ 1997, Westinghouse Electric Corporation.
July
6. NTD-NRC-95-4563, "GOTHIC Version 4.0 Documentation," September 21, 1995, Westinghouse Electric Corporation.
7. NTD-NRC-95-4577, "Updated GOTHIC Documentation," October 12, 1995, Westinghouse Electric Corporation.
8. NTD-NRC-95-4595, "AP600 WGOTHIC Comparison to GOTHIC," November 13, 1995, Westinghouse Electric Corporation.
9. R. P. Ofstun, "Experimental Basis for the AP600 Containment Vessel Heat and Mass Transfer Correlations," WCAP-14326, Rev. 1, May, 1997, Westinghouse Electric Corporation.
- * 10. F. E. Peters, "Final Data Report for PCS Large-Scale Tests, Phase 2 and Phase 3," WCAP-14135, ~~July 1994~~, Westinghouse Electric Corporation.
Rev. 1, April 1997
11. NUREG/CR-5809 EGG-2659, "An Integrated Structure and Scaling Methodology for Severe Accident Technical Issue Resolution," INEL, EG&G Idaho, Inc.
12. W. Wulff, "Scaling of Thermohydraulic Systems," BNL-62325, May 1995, Brookhaven National Laboratory.

Gilliland and Sherwood evaporation tests. These tests, as described in Reference 9, provided additional data to validate models for convective heat and mass transfer in AP600.

* Code capabilities have been examined using ~~both~~ ^{the} lumped parameter ~~and distributed parameter~~ formulations. The PCS test data and other data from the literature were used to provide input to code validation (Reference 4). The lumped parameter codes oversimplify the flow field by assuming a homogeneous mixture exists within each node. Since lumped parameter cannot resolve gradients within a node, effects such as stratification have been addressed external to the code to quantify the effects on AP600 containment pressure response. The use of the relatively large lumped parameter nodes in the AP600 evaluation model also overexpands an entering jet, leading to two competing effects on containment pressure calculation - overprediction of velocity and underprediction of steam concentration above the operating deck. The competing effects have been bounded (Reference 3) by utilizing only free convection heat and mass transfer on the inside of containment, which effectively eliminates the non-conservative velocity. This leaves only the underpredicted above-deck steam concentration which is itself conservative with respect to PCS heat removal.

* ~~Comparisons with LST data were also performed with calculations using the distributed parameter WGOTHIC formulation. The more detailed distributed parameter model (Reference 4, Appendix A) better represents phenomena, more closely matches the LST data, and helped confirm that phenomena occurring in the LST had been identified. The detailed distributed parameter model also confirmed the compensating errors in the lumped parameter model which were bounded in developing the evaluation model as discussed above. Because of practical computation limitations, it was elected to proceed with a bounding approach using the lumped parameter formulation of WGOTHIC.~~

Element 3 Assess Uncertainties and Develop Bounding Modeling Approaches

The results of scaling, testing, and code validation were used to establish a bounding analysis approach for each of the PIKT phenomena. Results of code validation and assessment of model uncertainties were used to develop a method of applying the WGOTHIC lumped parameter formulation to create a bounding DBA evaluation model using fixed noding. Sensitivity calculations (Reference 5, Section 5) were performed to gain insight into the influence of important parameters on the predicted pressure response. A key aspect of the evaluation model is that phenomena that are not part of the code calculation or are not well-represented within the code are evaluated separately and bounded by applying conservative boundary conditions or introducing biases into the evaluation model, as summarized in Section 2. The method used to address each phenomena in the evaluating model is documented in the PIRT (Reference 3).

The dimensionless groups needed to scale jet and plume momentum for their effects on stratification in the containment volumes are presented and relationships between AP600 and the LST are discussed in Section 6.5. The evaluation of stratification in compartments, and circulation between compartments, on AP600 to establish a bounding approach are documented in Reference 5, Section 9.

The momentum equation for the air flow through the PCS air flow path (downcomer, riser, and chimney) are developed, made dimensionless, and normalized to produce the pi groups required to scale momentum in the PCS air flow path.

The pi group values for the AP600 phenomena are evaluated, thereby providing a numerical basis for the importance of the dominant phenomena (transport processes and components) and validation of the PIRT rankings.

Scaled data from the SETs and IETs are compared to the scaling and phenomenological equations. The scaled tests are compared to AP600 to justify the use of the tests for evaluation model validation.

The rate of change equations for the containment gas mass, energy, and pressure are derived based on simple assumptions, using thermodynamic relationships, equation of state, and control volume conservation equations. The rate of change equations represent a single gas volume that is coupled to multiple heat sinks. The containment volume is assumed homogenous, except for the dead-ended compartments. The above-deck region is nearly homogeneous during and after blowdown due to the entrainment into the plume of more than 10 times its volumetric flow rate. The effect on heat sink utilization of deviations from a uniform vertical air/steam concentration distribution are shown to be minor (Reference 5, Section 9). *

The circulation and stratification report examines a range of break source momenta and directions, and shows that in all cases circulation between compartments maintains all but the dead-ended compartments at, or above the homogeneous steam concentration, and the above-deck region within 2 or 3 percent of the homogeneous concentration of approximately 60 percent steam. Although containment is not perfectly uniform, the deviations from homogeneous are small enough that the conclusions of the scaling analysis are valid.

The Westinghouse containment scaling analysis has evolved through a series of issued documents, presentations, and reviews. Extensive input has been received from the USNRC and the ACRS Thermal Hydraulics Subcommittee.

- Westinghouse issued Passive Containment Cooling System Preliminary Scaling Report, July 1994 (Reference 13)

2 DOMINANT PHENOMENA

The transport processes and components that affect containment pressure were identified and ranked according to importance in the PIRT. The phenomena ranked high and medium are the ones that receive more detailed treatment and validation, and should be addressed in the evaluation model. The phenomena ranked high or medium importance are listed in Table 2-1. The phenomena are organized according to whether they are represented by pi groups in the scaling analysis or whether the phenomena appear as parameters in pi groups. Those that appear as parameters are indented in the first column of the table, and identified as parameters in the column headed "PI Group." The high- and medium-ranked phenomena evaluated in this scaling analysis are identified in the column headed "Where Addressed." Many low importance phenomena are also addressed in this scaling analysis. High ranked phenomena not evaluated in this scaling analysis are briefly discussed and referenced to source documents at the end of this section.

The following high ranked phenomena are addressed by separate, detailed evaluations in which AP600 parameters were ranged to derive bounding inputs for the evaluation model.

- Circulation and Stratification - AP600 can be characterized by stratification within compartments and circulation between compartments. The scaling of jets and plumes, and the relationship of large-scale test (LST) stratification data to AP600 operation is presented in Section 6.5 of this document. The application of those data to AP600 is presented in Reference 5, Section 9. The circulation rates of air and steam between interconnected gas volumes (compartments) is addressed in Reference 5, Section 9.
- Intercompartment Flow - The mass flow rate of air and steam between interconnected gas volumes (usually referred to as circulation) affects heat sink utilization and is also addressed in Reference 5, Section 9.
- Source Fog - Source droplets (fog) occur during blowdown and increase the steam source density, thereby reducing its buoyancy. However, during blowdown, mixing inside containment is momentum- and pressure-dominated, not buoyancy-dominated. After blowdown, drops do not occur in the break source, so the post-blowdown source buoyancy is not affected. The effect of blowdown-generated drops on post-blowdown circulation is addressed in ~~the mixing and stratification report~~. However, the effect of droplets as heat sinks is addressed in this scaling document. *
Reference 5, Section 9, "Circulation and Stratification Within Containment"
- Liquid Film Stability - Liquid film stability affects the amount of surface area that can be covered by the PCS cooling water. In AP600, the time constant for heat transmission through the shell is relatively long, so the external surface temperature rises slowly relative to application of cooling water. Once the PCS water supply valve is opened, the water distribution weirs begin to fill and spill, leading to a development time for

Table 8-3 Containment and Heat Sink Mass Scaling Pi Group Values

Pi Group		Blowdown	Refill	Peak Press	Long Term	MSLB
Containment	τ_o (sec)	39	985	913	5173	537
	$\pi_{m,t}$	1.31	1.27	1.30	1.22	1.27
	$\pi_{m,brk}$	1.00	0.00*	1.00*	1.00	1.00
	$\pi_{m,i}$	1.75	0.00	2.00	0.00	0.00
Drops	$\pi_{m,flash,d}$	0.02	0.00	0.00	0.00	--
	$\pi_{m,evap,d}$	0.03	-0.04	0.01	0.00	--
Pool	$\pi_{m,p}$	0.04	0.00	0.03	0.07	--
Steel	$\pi_{m,st}$	-0.05	-1.41	-0.69	-0.02	-0.44
Concrete	$\pi_{m,cc}$	-0.01	-0.08	-0.02	-0.09	-0.12
Jacketed	$\pi_{m,jc}$	-0.02	-0.46	-0.23	-0.18	-0.08
Sc Shell	$\pi_{m,sc}$	--	--	-0.01	-0.06	--
Evap Shell	$\pi_{m,es}$	--	--	-0.43	-0.90	--
	$\pi_{m,esx}$	--	--	-0.02	-0.89	--
Dry Shell	$\pi_{m,ds}$	-0.02	-0.61	-0.03	-0.08	-0.37
Baffle	$\pi_{m,bf}$	0.00	0.00	0.00	0.00	--
Chimney	$\pi_{m,ch}$	0.00	0.00	0.00	0.05	--

* Refill was scaled with the same 200 lbm/sec flow rate used to normalize peak pressure.

Table 8-4 Containment and Heat Sink Energy Scaling Pi Group Values

Pi Group		Blowdown	Refill	Peak Press	Long Term	MSLB
Containment	$\pi_{e,t}$	0.55	0.58	0.56	0.63	0.58
	$\pi_{e,brk}$	1.00	0.00*	1.00*	1.00	1.00
	$\pi_{e,t,work}$	0.00	0.00	0.00	0.00	0.00
Drops	$\pi_{e,q,d}$	0.00	0.00	0.00	0.00	--
	$\pi_{e,jg,d}$	0.05	-0.04	0.00	0.00	--
Pool	$\pi_{e,q,p}$	0.00	0.00	0.00	0.00	--
	$\pi_{e,jg,p}$	0.03	0.00	0.02	0.06	--
Steel	$\pi_{e,q,st}$	0.00	-0.08	-0.03	0.00	-0.03
	$\pi_{e,jg,st}$	-0.05	-1.35	-0.64	-0.02	-0.44
	$\pi_{e,t,st}$	0.00	-0.05	-0.05	0.00	-0.01
Concrete	$\pi_{e,q,cc}$	0.00	0.00	0.00	0.00	-0.01
	$\pi_{e,jg,cc}$	-0.01	-0.07	-0.02	-0.08	-0.12
	$\pi_{e,t,cc}$	0.00	-0.01	0.00	-0.01	0.00
Jacketed Concrete	$\pi_{e,q,jc}$	0.00	-0.03	-0.01	0.00	-0.01
	$\pi_{e,jg,jc}$	-0.02	-0.44	-0.21	-0.16	-0.07
	$\pi_{e,t,jc}$	0.00	-0.02	-0.02	-0.02	0.00
Subcooled Shell	$\pi_{e,q,ss}$	--	--	0.00	0.00	--
	$\pi_{e,jg,ss}$	--	--	-0.01	-0.06	--
	$\pi_{e,t,ss}$	--	--	0.00	-0.01	--
	$\pi_{e,q,ssx}$	--	--	-0.01	-0.08	--
Evaporating Shell	$\pi_{e,q,es}$	--	--	-0.02	-0.03	--
	$\pi_{e,jg,es}$	--	--	-0.41	-0.81	--
	$\pi_{e,t,es}$	--	--	-0.02	-0.09	--
	$\pi_{e,q,esx}$	--	--	0.00	-0.03	--
	$\pi_{e,jg,esx}$	--	--	-0.02	-0.81	--
Dry Shell	$\pi_{e,q,ds}$	0.00	-0.03	0.00	0.00	-0.02
	$\pi_{e,jg,ds}$	-0.02	-0.59	-0.03	-0.07	-0.36
	$\pi_{e,t,ds}$	0.00	-0.02	0.00	-0.01	0.00
	$\pi_{e,q,dsx}$	0.00	0.00	0.00	-0.03	--

* Refill was scaled with the same pressure normalization used for peak pressure.

Table 8-4 Containment and Heat Sink Pressure Scaling Pi Group Values (cont.)

Pi Group		Blowdown	Refill	Peak Press	Long Term	MSLB
Chimney	$\pi_{e,q,ch}$	0.00	0.00	0.00	0.00	--
	$\pi_{e,fg,ch}$	0.00	0.00	0.00	-0.05	--
	$\pi_{e,l,ch}$	0.00	0.00	0.00	0.00	--
Baffle	$\pi_{e,q,bf}$	0.00	0.00	0.00	-0.02	--
	$\pi_{e,q,bfx}$	0.00	0.00	0.00	-0.02	--

* Refill was scaled with the same pressure normalization used for peak pressure.

Table 8-5 Containment and Heat Sink Pressure Scaling Pi Group Values

Pi Group		Blowdown	Refill	Peak Press	Long Term	MSLB
Containment	$\pi_{p,t}$	0.76	0.76	0.77	0.76	0.76
	$\pi_{p,g,brk,work}$	1.00	0.00*	1.00*	1.00	1.00
	$\pi_{p,g,brk,enth}$	0.03	0.00	0.03	0.02	0.03
	$\pi_{p,j,work}$	0.00	0.00	0.00	0.00	0.00
Drops	$\pi_{p,q,d}$	0.00	0.00	0.00	0.00	--
	$\pi_{p,enth,d}$	0.00	0.00	0.00	0.00	--
	$\pi_{p,work,d}$	0.05	-0.04	0.01	0.00	--
Pool	$\pi_{p,q,p}$	0.00	0.00	0.00	0.00	--
	$\pi_{p,enth,p}$	0.00	0.00	0.00	0.00	--
	$\pi_{p,work,p}$	0.04	0.00	0.03	0.07	--
Steel	$\pi_{p,q,st}$	-0.01	-0.24	-0.09	-0.00	-0.09
	$\pi_{p,enth,st}$	0.00	0.00	0.00	0.00	0.00
	$\pi_{p,work,st}$	-0.05	-1.41	-0.69	-0.02	-0.44
Concrete	$\pi_{p,q,cc}$	0.00	-0.01	0.00	-0.01	-0.02
	$\pi_{p,enth,cc}$	0.00	0.00	0.00	0.00	0.00
	$\pi_{p,work,cc}$	-0.01	-0.08	-0.02	-0.09	-0.12
Jacketed Concrete	$\pi_{p,q,k}$	0.00	-0.08	-0.03	-0.01	-0.02
	$\pi_{p,enth,k}$	0.00	0.00	0.00	0.00	0.00
	$\pi_{p,work,k}$	-0.02	-0.46	-0.23	-0.18	-0.08
Evaporating Shell	$\pi_{p,q,es}$	--	--	-0.07	-0.08	--
	$\pi_{p,enth,es}$	--	--	0.00	0.00	--
	$\pi_{p,work,es}$	--	--	-0.43	-0.90	--
Subcooled Shell	$\pi_{p,q,ss}$	--	--	0.00	0.01	--
	$\pi_{p,enth,ss}$	--	--	0.00	0.00	--
	$\pi_{p,work,ss}$	--	--	-0.01	-0.06	--
Dry Shell	$\pi_{p,q,ds}$	0.00	-0.10	-0.01	-0.01	-0.07
	$\pi_{p,enth,ds}$	0.00	0.00	0.00	0.00	0.00
	$\pi_{p,work,ds}$	-0.02	-0.61	-0.03	-0.08	-0.37

* Refill was scaled with the same pressure normalization used for peak pressure.

where the length parameter is the annulus hydraulic diameter, d_h . Incropera and DeWitt (Reference 32), Table 8.4, suggest the use of Colburn, Dittus-Boelter, and Seider-Tate correlations for internal flows.

- * The Dittus-Boelter correlation differs from Colburn by a Prandtl number exponent of 0.4 instead of $1/3$. For the predominantly air flows in the PCS, ^{the} Dittus-Boelter ~~gives results~~ correlation predicts heat transfer coefficients that are 2 percent ^{higher} ~~less~~ than Colburn.
- * The Seider-Tate correlation adds a multiplier of $(\mu/\mu_s)^{0.14}$ to the Colburn correlation. For the PCS with air and bulk-to-surface temperature differences less than 100°F , Seider-Tate ~~also gives results~~ ^{higher} correlation predicts heat transfer coefficients that are 2 percent ^{higher} ~~less~~ than Colburn.

All of these correlations are recommended for $Re > 10,000$, $L/D > 10$, and $.7 < Pr < 160$. The corresponding AP600 parameters are $16,100 < Re < 163,000$, $L/D = 60$, and $Pr = 0.72$ which satisfy the criteria for use of the Colburn correlation.

10.1.4 PCS Air Flow Path Flow Resistance

The natural circulation air flow rate in the PCS air flow path determines the riser Reynolds number, an important parameter in the evaporation mass transfer correlation. The PCS flow resistance is one of the dominant terms in the PCS momentum equation presented in Section 9. The form loss coefficient measurements from a geometrically scaled model of the AP600 PCS air flow path are presented and extrapolated to AP600.

The flow resistance in the PCS air flow path was measured in the $1/6$ scale air flow test (Reference 31). Although AP600 operates in natural circulation and the test was fan forced, the buoyant pressure, G_b , and the forced pressure drop, ΔP , are interchangeable in the pi groups. Consequently, a fan forced test produces a flow resistance that is equally valid for a buoyancy driven system.

The overall pressure loss coefficient for the system is a combination of form losses and friction losses. It is known from the test that the form and friction losses are approximately equal. Thus it is expected that the resistance should be a weak function of the Reynolds number, with an exponent on the Reynolds number approximately one-half the Reynolds number exponent for pure friction at the same Reynolds number. This can be demonstrated as follows.

Since form losses are known to be independent of Reynolds number at high Reynolds numbers ($K = C_1 Re^0$), and since the frictional losses are known to have only a weak dependence on Reynolds number at high Reynolds numbers ($fL/d = C_2 Re^n$, where $n = -0.20$), it is reasonable to expect the sum of the form and friction losses can also be approximated by a function of the form $K_{tot} = C_3 Re^m$. An approximating function can be defined as the

No Circulation Below-Deck - The lack of an opening between the simulated steam generator compartment and the other below-deck compartment that was open to the above-deck region prevented the above/below-deck circulation that would otherwise have developed. It also caused air-rich mixture below-deck and a steam-rich atmosphere above-deck. This, combined with other differences that affected heat sink effectiveness resulted in a distortion in the scaled transient pressure response in the LST. Consequently, circulation is a system level distortion.

The parameters that affect the mass transfer rate were measured and accounted for as parameters in the mass transfer correlation. Since the resulting range of independent variables in the test covered the range in AP600, as shown in Section 10.1, there is no distortion in the use of the LST as separate effects data. The LST data were further supplemented with data from international test at various larger scales to support the definition of a bounding approach for modeling the effects of internal circulation and stratification.

* External Water Flow too High - The energy and pressure scaling pi groups for the subcooled shell presented in Tables 8-4, 8-5, and ~~8-6~~³ all show subcooled heat transfer effects are second-order phenomena. Consequently any differences between the test and AP600 values have only a minor effect on the system pressure response and thus are not system-level distortions.

* The results of scaling test 213.1C presented in Table ~~8-3~~³ show the measured value of $\pi_{e,q,ssx}$ is less than the calculated value for AP600. Consequently, the amount of heat removed by the subcooled liquid in the LST is not always greater than in AP600. There are, of course other tests with higher external water flow rates in which the LST scaled heat removal is greater than that in AP600. Since the flow rates were not all too high, the effect is that of a ranged parameter, and is neither a difference nor a distortion.

External Water Flow Was Established Before Break - The external water flow is one of several external processes that combined to produce the rate of heat removal from the containment gas. Since the system level pressure and scaled dominant variables are distorted, it is likely that the external water flow contributed to the distortion.

Two tests were conducted that had cold water applied to a hot shell. LST 219.1 operated at a dry steady state shell temperature of 240°F, then water was applied. One shakedown test was operated at 250°F shell temperature, then water was applied while the process was video taped. These tests provided separate effects test data and behavior to support the validation of the external wetting and stability model.

Table 2-1 Phenomena Identification and Ranking Table - Summary of High and Medium Ranked Phenomena

Phenomenon *	Effect on Containment	Pi Groups	Where Addressed
* Break Source Mass and Energy (1A) and Liquid Flashing (1B) and Evaporation (5B)	The only mass and energy source for containment pressurization	$\pi_{p,g,brk,enth}$ $\pi_{p,g,brk,work}$ $\pi_{p,work,d}$ $\pi_{p,work,p}$	Scaling Analysis
Gas Compliance (2C)	Stores mass and energy in atmosphere, increasing pressure	$\pi_{p,t}$	Scaling Analysis
Initial Conditions Inside (4A, 4B, 4C)	Temperature, humidity, pressure affect noncondensables and energy storage	None	Initial Conditions Ref. 5, Section 5
Containment Solid Heat Sinks (3), Pool (5), Drops (1), and Shell (7)	Store energy (and remove mass from atmosphere) reducing pressure	$\pi_{p,i}$ $\pi_{p,work,j}$	Scaling Analysis *
* Internal Heat Sink Conduction (3D, 5E, 7) and Heat Capacity (3E, 5) (7G, 1E)	Limits conduction heat transfer into heat sinks, shell, or pool, and through shell. Stratification in the break pool can affect the effective heat capacity of the pool.	parameter	Scaling Analysis
Heat Transfer Through Horizontal Liquid Films	Water and noncondensable layers on upward facing horizontal surfaces limit heat and mass transfer to horizontal heat sinks	parameter	Scaling Analysis
Condensation Mass Transfer (3F, 5G, 7C)	The single first-order transport process that removes mass and energy from the containment gas	$\pi_{p,work,j}$	Scaling Analysis
* Break Source Direction and Elevation (1B), Momentum (1C), Density (1D) and Droplets (1E)	Direction, elevation, density, and momentum can dominate circulation and affect condensation rate. Existence of droplets in source during blowdown affects the effective source density.	parameter	Circulation and Stratification, Ref 5, Section 9
Circulation and Stratification	Intercompartment Flow (Circulation) and stratification can affect the distribution of steam near heat sinks for condensation heat removal. Rising liquid level blocks lower circulation flow paths	parameters	
Intercompartment Flow			
* Break Pool Flooding Level (5F)			
Source Fog (3H)	Affects circulation and stratification via buoyancy	parameter	

Table 2-1 Phenomena Identification and Ranking Table - Summary of High and Medium Ranked Phenomena (cont.)			
Phenomenon *	Effect on Containment	Pi Groups	Where Addressed
Evaporation Mass Transfer (7A)	The first-order transport process that removes mass and energy from the evaporating external shell	$\pi_{e,fg,esx}$	Scaling Analysis
PCS Natural Circulation (7A)	Convective air flow provides convective heat and mass transfer from containment shell.	parameter	Scaling Analysis
Liquid Film Flow Rate (7A), Water Temperature (7A), Film Stability (7A)	Affects the upper limit for water coverage on the external shell	parameter	Film Stability, Ref. 5, Section 7
* Liquid Film Energy Transport (3A)	<i>Inside:</i> Carries 14 percent of condensation energy to the IRWST and break pool. <i>Outside:</i> Absorbs 8 percent of energy rejected by the external shell surface.	$\pi_{e,i,j}$ See note 1 $\pi_{e,q,ssx}$	Scaling Analysis
* Convection Heat Transfer (7A), (14A)	A second order transport process that removes energy from the containment gas, and from the external shell.	$\pi_{p,q,j}$ $\pi_{e,q,esx} + \pi_{e,q,dx}$ Note 2	Scaling Analysis
* Radiation Heat Transfer (7A)	A second order transport process that removes energy from the containment gas and from the external shell.	$\pi_{p,q,j}$ $\pi_{e,q,esx} + \pi_{e,q,dx}$ Note 2	Scaling Analysis
Baffle Conduction (7A) and Baffle Leakage paths (10G)	Conduction through the baffle into downcomer volume and leakage paths can influence the external natural circulation flow rates	$\pi_{e,q,bf}$ $\pi_{e,q,bfx}$ None for leakage	PIRT Sections 4.4.10D and 4.4.10G

* Indicators in parentheses refer to phenomena in the "Phenomena Identification and Ranking According to Effect on Containment Pressure" (Reference 3, Table 4-1).

Note 1. The fraction of the internal condensation energy carried away by the liquid film is defined by the ratio: $\pi_{e,i,j} / (\pi_{e,i,j} + \pi_{e,fg,j})$, for each heat sink j. The fraction of the external shell heat rejection that goes into the subcooled heat capacity of the external liquid is defined by the ratio: $\pi_{e,q,ssx} / (\pi_{e,q,ssx} + \pi_{e,q,esx} + \pi_{e,fg,esx} + \pi_{e,q,dx})$. The pi group values for AP600 are presented in Section 8.

Note 2. Inside containment $\pi_{p,q,j}$ represents the pressure effect of sensible heat transfer. The sensible heat transfer is approximately 1/2 radiation heat transfer and 1/2 convection heat transfer. Outside containment $\pi_{e,q,esx} + \pi_{e,q,dx}$ represents the sum of the dry and evaporating shell sensible heat transfer, that is approximately 1/2 radiation heat transfer and 1/2 convection heat transfer.

2. (RAI 480.995) In the previous revision of the scaling report, the Biot number had been calculated to be 0.08. Now it has been recalculated as 0.13. According to Kreith, "Principles of Heat Transfer," 3rd ed., p. 140, a criterion for treating a heat structure as a lumped mass is that the Biot number be less than 0.1. Since Kreith's criteria is no longer satisfied, what is the justification for lumping the steel? What is the magnitude of the error introduced by this approximation?

RESPONSE:

Kreith's Biot criteria $Bi < 0.1$ is based on a temperature error of less than 5%. It is estimated that $Bi < 0.13$ would give a temperature error of less than 10%. Such an error is considered acceptable for a scaling analysis in view of the simplicity of the lumped parameter assumption.

To clarify the use of Biot numbers $Bi < 0.13$, the first paragraph of Section 7.5.5, "Steel Thermal Model," WCAP-14845, Rev. 2, "Scaling Analysis for AP600 Containment Pressure During Design Basis Accidents," will be deleted and replaced with the following:

"The average steel thickness, calculated from the steel volume/area (Section 3) is 0.4 inches. The Biot number for steel of the average thickness is $Bi = 0.13$. From Kreith's text (Ref. 20), a Biot number of $Bi = 0.1$ is noted to result in a maximum temperature error of no more than 5%. It is estimated that a Biot number of $Bi < 0.13$ will result in a maximum temperature error of no more than 10%. Such an error is considered acceptable for a scaling analysis in view of the simplicity of the lumped parameter assumption. Thus, the steel can be modeled as a lumped mass and $T_{surf} = T_m$ in Equation (118). With this assumption, the surface heat flux and total stored energy in the heat sink can be related to the heat sink surface temperature and average temperature."

and the external film outer surface with convection heat transfer and evaporation to the riser bulk flow, and radiation to the baffle is:

$$T_{xf,s} - T_{ri} = \dot{q}_{out}'' \left(h_{mx} + h_{cx} + h_{rx} \frac{(T_{xf,s} - T_{bf})}{(T_{xf,s} - T_{ri})} \right)^{-1} \quad (132)$$

These two equations are added, resulting in the equation:

$$(T_{sh,o} - T_{ri}) = \dot{q}_{out}'' \left[(h_{xf})^{-1} + \left(h_{mx} + h_{cx} + h_{rx} \frac{(T_{xf,s} - T_{bf})}{(T_{xf,s} - T_{ri})} \right)^{-1} \right] \quad (133)$$

The term in brackets is the inverse conductance for the outside of the shell, where the conductance is $h_{ex,o}$. Equations (130) and (133) can be combined with the general energy equation for a heat sink, Equation (90), to give:

$$m_{sh} c_{v,sh} \frac{dT_{sh}}{dt} = h_e A (T - T_{sh,i}) - h_{ex} A (T_{sh,o} - T_{ri}) \quad (134)$$

Equation (134) was written for the evaporating portion of the shell, but is also valid for the subcooled and dry portions of the external shell, with substitutions for the subcooled region $h_{mx} = h_{cx} = h_{rx} = 0$, and for the dry portion $h_{xf} = h_{mx} = 0$.

The areas of the subcooled and evaporating regions can vary with time, so a basis for calculation is required. The area of the subcooled region is determined from an energy balance on the subcooled liquid in which the heat conducted from the shell heats the liquid from its source temperature to the temperature of the evaporating film, T_{xf} . The subcooled film is assumed to have no evaporation, radiation, or convection from its surface. The bases for this assumption are:

- The subcooled water exists at the top of the shell where the riser temperature is at its maximum. When compared to the average subcooled film temperature, $T_{xf,avg} = (T_{in} + T_{xf})/2$, the difference $(T_{xf,avg} - T_{ri})$ is a small positive value at peak pressure, and a small negative difference at long-term pressurization.
- The subcooled surface area is relatively small, only a few percent of the total, so errors have little effect on the evaporating region where most of the shell heat is removed.

The calculation proceeds by calculating the temperature of the evaporating film, $T_{xf,s}$, as shown in Figure 7-3. The water flowing over the subcooled shell surface area, A_{sc} is assumed to heat linearly from the ~~film~~ source temperature, T_{in} to $T_{xf,s}$. The average subcooled film temperature is then $T_{sc,avg} = (T_{in} + T_{xf,s})/2$. A simple energy balance on the

subcooled film can be written relating the sensible temperature rise of the film to the energy conducted into the film from the shell. That is, $\dot{m}_{xf} c_V (T_{xf} - T_{in}) = h_{xf} A_{sc} (T_{xf,avg} - T_{sc})$. The subcooled film conductance is defined in Equation (142). The subcooled film area is estimated by rearranging this energy balance.

$$A_{sc} = \frac{\dot{m}_{xf} c_V (T_{xf} - T_{in})}{h_{xf} (T_{ssx} - T_{xf,avg})} \quad (155)$$

The liquid film wetted surface area is then estimated as discussed in Section 7.6.6, and the evaporating area is the difference between the wet area and the subcooled area,

$$A_{evap} = A_{wet} - A_{sc} \quad \text{The dry area is the difference between the total area and the wet area,}$$

$$A_{dry} = 52662 \text{ ft.}^2 - A_{wet}$$

7.6.1 Shell Conductance

The individual conductance terms inside the shell are free convection heat and mass transfer, radiation, and liquid film conduction. These are evaluated independently for the internal portions of the shell that correspond to the subcooled, evaporating, and dry portions of the external shell.

$$h_m = \frac{0.13 (h_g - h_f) \rho_{stm} D_v \Delta P_{stm}}{(T - T_{if}) (v^2 / g)^{1/3} P_{lm,air}} \left(\frac{\Delta \rho}{\rho} Sc \right)^{1/3}$$

$$h_c = \frac{0.13 k}{(v^2 / g)^{1/3}} \left(\frac{\Delta \rho}{\rho} Pr \right)^{1/3} \quad (136)$$

$$h_r = \sigma \epsilon f(T, T_{if}) \quad h_{if} = k_{if} / \delta_{if}$$

$$h_e = [(h_m + h_c + h_r)^{-1} + h_{if}^{-1}]^{-1}$$

The conductance pi groups are each of these values divided by the reference shell conductance for each of the three shell portions. The fifteen pi groups result:

$$\begin{aligned}
 \pi_{c,e,sc} &= \frac{h_{e,sc,o}}{h_{sh,o}} & \pi_{c,m,sc} &= \frac{h_{m,sc,o}}{h_{sh,o}} & \pi_{c,c,sc} &= \frac{h_{c,sc,o}}{h_{sh,o}} & \pi_{c,r,sc} &= \frac{h_{r,sc,o}}{h_{sh,o}} & \pi_{c,if,sc} &= \frac{h_{if,sc,o}}{h_{sh,o}} \\
 \pi_{c,e,es} &= \frac{h_{e,es,o}}{h_{sh,o}} & \pi_{c,m,es} &= \frac{h_{m,es,o}}{h_{sh,o}} & \pi_{c,c,es} &= \frac{h_{c,es,o}}{h_{sh,o}} & \pi_{c,r,es} &= \frac{h_{r,es,o}}{h_{sh,o}} & \pi_{c,if,es} &= \frac{h_{if,es,o}}{h_{sh,o}} \\
 \pi_{c,e,ds} &= \frac{h_{e,ds,o}}{h_{sh,o}} & \pi_{c,m,ds} &= \frac{h_{m,ds,o}}{h_{sh,o}} & \pi_{c,c,ds} &= \frac{h_{c,ds,o}}{h_{sh,o}} & \pi_{c,r,ds} &= \frac{h_{r,ds,o}}{h_{sh,o}} & \pi_{c,if,ds} &= \frac{h_{if,ds,o}}{h_{sh,o}}
 \end{aligned}
 \tag{137}$$

The evaporating portion of the shell outside operates with forced convection heat and mass transfer, radiation, and liquid film conductance:

$$h_{m,ex} = \frac{0.023 h_{fg} \rho_{stm} D_v \Delta P_{stm}}{(T - T_{xf}) d_h P_{lm,air}} Re_d^{0.8} Sc^{1/3}$$

$$h_{c,ex} = \frac{0.023 k}{d_h} Re_d^{0.8} Pr^{1/3}$$

(138)

$$h_{r,ex} = \sigma \epsilon f(T_{xf} T_{bf})$$

$$h_{xf,ex} = k_{yf} / \delta_{xf}$$

$$h_{ex} = \left[\left(h_{mx} + h_{cx} + h_{rx} \frac{\left(\frac{T_{dew}^{xf} - T_{bf}}{T_{dew}^{xf} - T_n} \right)^{-1}}{\left(\frac{T_{dew}^{xf} - T_n}{T_{dew}^{xf} - T_{bf}} \right)^{-1}} \right) + h_{xf}^{-1} \right]^{-1}$$

The method used to calculate the evaporating, subcooled and dry areas is:

- Calculate the subcooled area as described in Section 7.6 and Equation (135).
- Subtract the subcooled area from the maximum wet area ($44,596 \text{ ft}^2 - A_{sc}$) to get the maximum evaporating area. *
SSX
- Use the maximum evaporating area to calculate the total evaporation. If the total evaporation is greater than 40 lbm/sec (Reference 5, Table 7-9, peak heat flux) then reduce the evaporating area until the evaporation rate is 40 lbm/sec.
- Subtract the evaporating area and the subcooled area from the total area to get the dry area $A_{dry} = 52,662 \text{ ft}^2 - A_{sc} - A_{evap}$. *
SSX

7.7 BAFFLE ANALYSIS AND SCALING EQUATIONS

The baffle receives heat by radiation from the shell and loses heat by radiation to the shield building and by convection to the riser and downcomer. The energy equation for the baffle is formulated accordingly, assuming radiation heat transfer from both wet and dry portions of the shell that are generally at different temperatures. Examination of when the shell becomes wetted, and the temperatures calculated for the wet and dry portions of the shell shows that through the beginning of the peak pressure time phase, the outer shell temperatures for wet and dry portions are sufficiently close in temperature that wet or dry does not matter. Furthermore, once wetting is well along, the shell heat rejection to the baffle can be minimized by assuming 100 percent of the shell is wet (although for shell evaporative heat losses to the riser a lesser fraction is assumed wet). For the scaling analysis the baffle was forced by the dry shell during blowdown and refill, and by the wet shell from the beginning of the peak pressure period and beyond.

The baffle is a thin steel member with a Biot number, based on the inside surface maximum dry heat transfer coefficient of $11 \text{ B/hr-ft}^2\text{-F}$, of 0.0044. Even with condensation h is approximately $100 \text{ B/hr-ft}^2\text{-F}$ and $Bi = 0.04$. Both of these values are small enough that the baffle is well-represented as a lumped mass with identical bulk and surface temperatures. Both sides of the baffle are subject to forced convection and radiation. The downcomer side of the baffle is always dry. The riser side of the baffle may be wet or dry, depending upon the radiation heat transfer rate to the baffle and the convection heat transfer from the baffle to the riser and downcomer. The energy equation for the baffle is:

$$\begin{aligned}
 m_{bf} c_v \frac{dT_{bf}}{dt} = & h_{r,shx-bf} A (T_{shx} - T_{bf}) + h_{c,ri-bf} A (T_{ri} - T_{bf}) - h_{r,bf-dc} A (T_{bf} - T_{dc}) \\
 & - h_{c,bf-dc} A (T_{bf} - T_{dc}) + \dot{m}_{stm,bf} h_{fg}
 \end{aligned} \quad (156)$$

In terms of inside and outside equivalent conductances, the baffle equation is:

$$m_{bf} c_v \frac{dT_{bf}}{dt} = h_e A_{bf} (T_{ri} - T_{bf}) - h_{ex} A_{bf} (T_{bf} - T_{dc}) \quad (157)$$

7.7.1 Baffle Conductance

The individual baffle conductance terms are:

$$\begin{aligned}
 h_{r,shx-bf} &= \sigma \epsilon f(T_{shx}, T_{bf}) & h_{r,bf-dc} &= \sigma \epsilon f(T_{bf}, T_{dc}) \\
 h_{m,ri-bf} &= \frac{h_{fg} \rho_{stm} D_v}{(T_{ri} - T_{bf}) d_h} \frac{\Delta P_{stm}}{P_{lm,air}} 0.023 Re_d^{0.8} Sc^{1/3} \\
 h_{c,ri-bf} &= \frac{k}{D_h} 0.023 Re_d^{0.8} Pr^{1/3} & h_{c,bf-dc} &= \frac{k_o}{d_h} 0.023 Re_{d,o}^{0.8} Pr_o^{1/3}
 \end{aligned} \quad (158)$$

$$h_e = h_{m,ri-bf} + h_{c,ri-bf} + h_{r,shx-bf} \frac{(T_{shx} - T_{bf})}{(T_{ri} - T_{bf})} \quad h_{ex} = h_{c,bf-dc} + h_{r,bf-dc}$$

* Both ^t the riser ~~operating in forced convection~~ and the downcomer ~~in opposite mixed convection~~ consistent with the results shown in Figure 4-i. The liquid film conductance on the baffle is neglected.

The individual conductance terms are normalized to the shell conductance, $h_{sh,o}$, to produce the pi groups for scaling the heat sink conductances:

5. (RAI 480.1017) The RAI was directed toward determining whether any of the remaining pi-group values contained an anomaly similar to that for $pi_{c, bf}$. The NRC review did not check the value of every pi-group. Please provide an evaluation of the anomaly effect for $pi_{c, dry}$ and $pi_{c, wet}$.

RESPONSE:

Note: Previously, a response to this question was prepared that included two paragraphs followed by a table, followed by another sentence in bold letters. The complete response to this item keeps the first two paragraphs and the table, titled "Table 1 -- Temperature Differences and Heat Transfer Coefficients for the Shell and Baffle." The following text is to be inserted immediately following Table 1 of the previous response.

Insert after "Table 1 -- Temperature Differences and Heat Transfer Coefficients for the Shell and Baffle."

Westinghouse will delete the last paragraph in Section 8.2, "Conductance PI Group Values," of WCAP-14845, Revision 2, "Scaling Analysis for AP600 Containment Pressure During Design Basis Accidents," and replace it with the following text.

The remaining conductances range from 0.01 to 0.05. These are small values, mainly because mass transfer is not involved with the energy transport associated in these regions. The chimney operates with low conductances, even when condensate forms, due to the high non-condensable concentration in the adjacent air flow. The dry shell external conductance is 1 to 2 orders of magnitude less than the internal conductance associated with the internal shell.

The outside and inside baffle surfaces both operate dry and, consequently, have low conductances. The low values are indicative of the small energy transport associated with these surfaces. Furthermore, the energy transport processes across the two surfaces are similar in magnitude and should have similar conductance ratios for all time periods during transient. The negative conductance ratio calculated for baffle inside surface during the long term portion of the transient is the result of an unfortunate selection in temperature difference for normalizing the conductance. This negative value is not meaningful for comparison purposes and should be ignored.

7. (RAI 480.1027) In addition to the information in the RAI, the following is needed to complete the review. Please compare the physical film thickness (as predicted by the Nusselt equation) to the Chun and Seban effective film thickness over the range of Reynolds Numbers expected for the AP600 (both inside and outside the PCS, above and below the second weir). For each Reynolds Number, compare the heat transfer coefficient for the water film using the Nusselt model and the Chun and Seban model.

The wording in the first paragraph of Section 7.4 has been improved to distinguish the effective film thickness from the physical film thickness. Unfortunately, in the second paragraph, the effective film thickness is used to get the heat capacity of the film, whereas the physical thickness should be used. The difference in the ratio calculated is not significant, but it confuses the issue, in the sense that it encourages the reader to think of the effective thickness as a physical distance.

RESPONSE:

First two paragraphs of existing response as good as is.

The condensation heat transfer data of Kutateladze et al. for working fluids of refrigerant 12 ($Pr = 3.5$) and refrigerant 21 ($Pr = 3.06$) is added to the graph given in Figure 3.10-1. This amended figure is attached. Also, the following text will be added to the text of section 3.10, "Chun and Seban Liquid Film Conductance Model," of WCAP-14326, Revision 1:

See marked-up page that is attached.

Insert 3: Kutateladze et al. determined the heat transfer coefficients for two working fluids in film condensation on vertical surfaces⁽²⁵⁾. These two sets of data are also plotted on Figure 3.10-1 and are nominally identified as having Prandtl numbers of 3.06 (actual range of 2.74 to 3.06) and 3.5 (actual range 3.14 to 3.52). At lower Reynolds numbers, $Re < 100$, the Chun and Seban correlation provides an upper bound to data for both working fluids. Between the range of $100 < Re < 400$, the Chun and Seban correlation provides a "best estimate" fit to the data. In the range of $400 < Re < 2000$, Nusselt numbers given by the Chun and Seban Wavy Laminar Correlation are lower than (conservative relative to) the data reported in Reference 25.

Insert 4: Using the AP600 containment Evaluation Model's minimum liquid film flow rate of $\Gamma_{MIN} = 120$, a minimum evaporating film Reynolds number of about 700 is calculated. Comparing the Chun and Seban correlation to the data above this Reynolds number, the correlation is observed to be a good fit to the evaporation data and conservative relative to the condensation (lower than the data).

Also, the list of references will be amended to include the following:

REFERENCES

25. Kutateladze, S. S., Gogonin, I. I., Grigo'eva, N. I. and Dorokhov, A. R. "Determination of Heat Transfer Coefficient with Film Condensation of Stationary Vapour on a Vertical Surface," *Thermal Engineering*, Volume 24, Number 4, pp 184-186 (1980).

The Chun and Seban correlation is compared to the Chun and Seban data for evaporating films and to data for condensing films from

3.10 Chun and Seban Liquid Film Conductance Model⁽⁷⁾

by K. K. Kellogg⁽²⁴⁾ and [unclear]

presented in Figure 3.10-1

H ① The Chun and Seban correlation is used to predict heat transfer through the condensing and evaporating liquid films. The correlation applies to both turbulent and wavy laminar films, and was compared to data in the original paper. Data from tests at the University of Wisconsin⁽²³⁾ extend the validity of the Chun and Seban correlation to condensing wavy laminar flow and to surfaces that are inclined as in the dome region of the AP600.

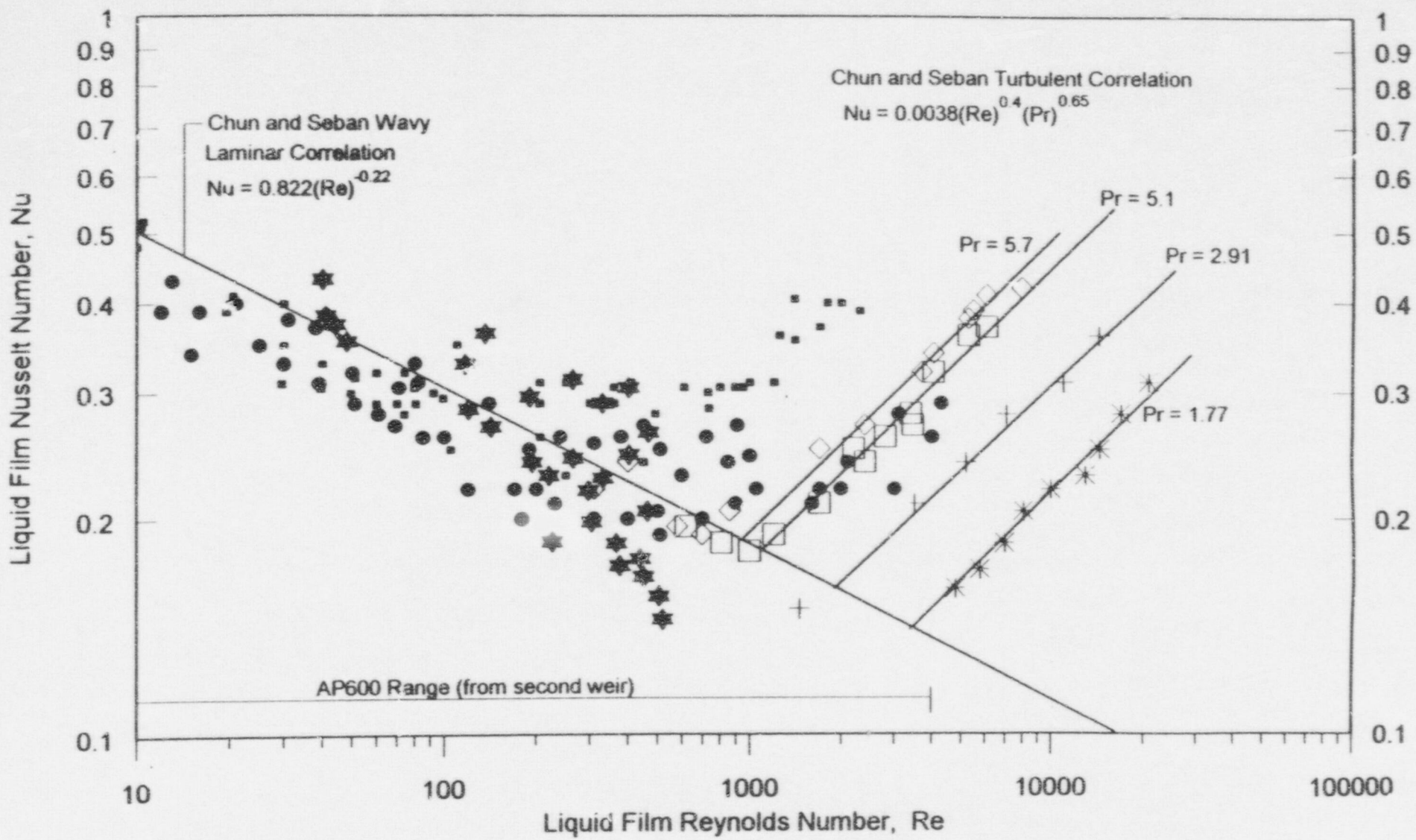
6, 12, 45, and 88 degrees from horizontal to simulate

H ⑤ The Wisconsin test facility is described in Section 3.8. Five of the Wisconsin⁽²³⁾ tests (95 through 99) were conducted without a noncondensable gas present. Without a noncondensable gas, the gas-to-liquid heat transfer coefficient is so high that the gas-to-liquid temperature drop is negligible compared to the temperature drop across the liquid film. Consequently, the temperature of the liquid film surface may be assumed equal to the gas temperature and the liquid film heat transfer coefficient can be calculated from the heat flux divided by the liquid film temperature drop. Since the heat flux, solid surface temperature, and liquid film surface temperature are known, the heat transfer coefficient may be derived directly from the measurements. The Wisconsin tests thus provided a direct indication of the liquid film heat transfer coefficient for a range of surface inclinations from vertical to horizontal, covering a range of film Reynolds number in the wavy laminar regime.

~~The Wisconsin⁽²³⁾ and Chun and Seban⁽⁷⁾ data are compared to the Chun and Seban laminar and turbulent correlations in Figure 3.10-1. The correlation predicts nearly best-estimate values over the full Reynolds number range of data. The range of film Reynolds numbers on the outside of AP600 is also shown in the figure and falls well within the range of the test data. Reynolds numbers on the inside of containment are less than outside due to film removal at the crane rail and stiffener ring and the fact that the inside film flow rate starts at zero at the top of the dome and increases as the film flows down. The AP600 liquid film Prandtl number range is approximately $1.5 < Pr < 3.0$, whereas the range of the Chun and Seban data Prandtl numbers is $1.77 < Pr < 5.9$, which adequately covers the AP600 range. Comparison of the correlation to the test data show that the Chun and Seban correlation is a good, best-estimate representation of the data.~~

② *after from these*
We see the external flow starts high at the top and reduces due to evaporation down the side walls.

H ⑥ The large scatter in the Wisconsin⁽²³⁾ liquid film heat transfer data is believed to result from operating the tests at (or beyond) the range of operation for which the test facility was designed. The presence of even small amounts of noncondensable gases would bias the results.



Wisconsin Pr = 1.77	Chun & Seban Pr = 5.7	Chun & Seban Pr = 5.1	Chun & Seban Pr = 2.9	Chun & Seban Pr = 1.77	Kutateladze Pr = 3.06	Kutateladze Pr = 3.5
★	◇	□	+	*	●	•

8. (RAI 480.1031) In Table 10-3 the new footnote reveals that for LST, measured air/steam concentrations were used since LST is not homogeneous. How were the air steam concentrations for AP-600 determined for use in calculating the pi-group?

RESPONSE:

Five cases of the rising plume from the break mixing with containment atmosphere were evaluated in Section 9.C.1.4. For the case of the weak (minimal entrainment) plume the variation in relative steam concentration from top to bottom along the vertical containment shell is calculated to be no more than 0.073. Thus, for practical purposes, model predicts the containment atmosphere maintains a relatively uniform steam concentration.

Section 1.2 of WCAP-14845, Revision 2, "Scaling Analysis for AP600 Containment Pressure During Design Basis Accidents" states the well-mixed air/steam containment atmosphere is assumed. To provide a basis for this assumption, page 1-5 of Section 1.2, WCAP-14845, Revision 1, will be amended as shown in the attached mark-up to reference Section 9.C.1.4 of WCAP-14407, Revision 1, "WGOthic Application to AP600."

The following will be appended as footnote (4) to the column labeled "AP00" in Table 10-3 of WCAP-14845, Revision 2, "Scaling Analysis for AP600 Containment Pressure During Design Basis Accidents,"

- (4) Predicted using uniform air/steam concentrations as stated in Section 1.2, page 1-5 of this report.

The dimensionless groups needed to scale jet and plume momentum for their effects on stratification in the containment volumes are presented and relationships between AP600 and the LST are discussed in Section 6.5. The evaluation of stratification in compartments, and circulation between compartments, on AP600 to establish a bounding approach are documented in Reference 5, Section 9.

The momentum equation for the air flow through the PCS air flow path (downcomer, riser, and chimney) are developed, made dimensionless, and normalized to produce the pi groups required to scale momentum in the PCS air flow path.

The pi group values for the AP600 phenomena are evaluated, thereby providing a numerical basis for the importance of the dominant phenomena (transport processes and components) and validation of the PIRT rankings.

Scaled data from the SETs and IETs are compared to the scaling and phenomenological equations. The scaled tests are compared to AP600 to justify the use of the tests for evaluation model validation.

The rate of change equations for the containment gas mass, energy, and pressure are derived based on simple assumptions, using thermodynamic relationships, equation of state, and control volume conservation equations. The rate of change equations represent a single gas volume that is coupled to multiple heat sinks. The containment volume is assumed homogenous, except for the dead-ended compartments. The above-deck region is nearly homogeneous during and after blowdown due to the entrainment into the plume of more than 10 times its volumetric flow rate. The effect on heat sink utilization of deviations from a uniform vertical air/steam concentration distribution are shown to be minor (Reference 4, 5 Section 9).

The circulation and stratification report examines a range of break source momenta and directions, and shows that in all cases circulation between compartments maintains all but the dead-ended compartments at, or above the homogeneous steam concentration, and the above-deck region within 2 or 3 percent of the homogeneous concentration of approximately 60 percent steam. Although containment is not perfectly uniform, the deviations from homogeneous are small enough that the conclusions of the scaling analysis are valid. (5)

The Westinghouse containment scaling analysis has evolved through a series of issued documents, presentations, and reviews. Extensive input has been received from the USNRC and the ACRS Thermal Hydraulics Subcommittee.

- Westinghouse issued Passive Containment Cooling System Preliminary Scaling Report, July 1994 (Reference 13)

Internal Heat Sinks Not Prototypic - The scaling analysis shows the net heat sink performance in the LST is not distorted during the early portion of a blowdown or during steady-state operation, but is distorted between these times.

Condensation and heat transfer to the shell were characterized using detailed local measurements in a separate effects mode. The different internal heat sinks in the LST did not affect the validity of the condensation separate effects data.

External Water Flow Time Variations - The external water supply rate varied with time. The flow rate dropped when the boiler feed-water level initiated refill of the feedwater tank, temporarily reducing the external water flow rate. The cycling rate was proportional to the steam flow rate, and was typically on the order of a few minutes. The reduced flow portion of the cycle was only a fraction of the total cycle, with the majority of the cycle operating at the set flow rate. The flow cycling may have had a minor effect on the vessel cooling and water coverage. Since all but two tests operated with significantly more flow than could evaporate, the flow fluctuations had little effect on cooling. Consequently, the external water flow variation is not a distortion.

The separate effects test data used to validate the heat and mass transfer models used time and spatial-averaged temperatures, flow rates, and fluxes. The averaging time period was long enough to include several cycles, so fluctuations are averaged out. Furthermore, the transport models include data from other tests that did not experience such fluctuations. The fluctuations are not believed to have affected vessel cooling in a way that could compromise the use of the LST for pressure, temperature, or transport predictions.

The external water flow rate is a relatively steady flow, interrupted by a periodic drop and recovery. Since the water coverage increases with time, the flow fluctuations prevent the coverage from reaching the maximum possible steady flow value. The separate effects data were evaluated using both the maximum and minimum flow rates, so a conservative approach was used for the data evaluation, ^{as described in Reference 5, section 7.6.3.} Although the flow variations are considered a distortion in the separate effects data, the use of maximum and minimum flow rates for data correlation adequately compensates. The film stability model uses a bounding approach that bounds both the maximum and minimum data for film stability. *

Crane Rails Are Not the Same - The LST lacked an internal structure to simulate the stiffener ring located part-way up the vessel side wall. The crane rail and stiffener ring strip the liquid film flowing down the inside surface. The film redevelops below these structures. The stripped film is thinner and has a higher conductance than a film that is not stripped, but both conductances are so high they have little effect on AP600 performance. Since the scaling analysis showed the film conductance was less than second order, relative to the other conductances, incomplete simulation in the test has an insignificant effect on the results so is not a distortion at either the system level or component level.

**Additional Markups to WCAP-14845 Rev 2, "Scaling Analysis for AP600 Containment
Pressure During Design Basis Accidents"**

The term that is of interest for scaling is the pool evaporation rate term. That term is normalized by the break steam flow rate and made dimensionless with the variable

$$\dot{m}_{\text{evap,p}} = \dot{m}_{\text{evap,p,o}} \dot{m}_{\text{evap,p}}^*$$

$$\frac{\dot{m}_{\text{evap,p,o}}}{\dot{m}_{\text{g,brk,o}}} = \frac{\dot{m}_{\text{evap,p,o}} \dot{m}_{\text{evap,p}}^*}{\dot{m}_{\text{g,brk,o}}} = \pi_{\text{m,evap,p}} \dot{m}_{\text{evap,p}}^*$$

(108)

$$\text{where } \pi_{\text{m,p}} = \frac{\dot{m}_{\text{evap,p,o}}}{\dot{m}_{\text{g,brk,o}}}$$

The effect of the pool on containment pressure is maximized by assuming the liquid enters at the containment saturation temperature, similar to drops. During the peak pressure and long-term time phases, saturated break liquid is assumed to flow across the top of the pool and to cool as it spreads. The net evaporation rate is the integrated evaporation flux over the surface area. The pool surface temperature was assumed to be at a steady-state with the spreading layer evaporating to the atmosphere, but not mixing or conducting to the cooler layer below. This maximizes the evaporation rate, resulting in the maximum pressure effect. The resulting evaporation rates are presented in Table 7-2 for the peak pressure and long-term time phases.

During blowdown the high velocity jet and spray are assumed to produce sufficient liquid surface area to result in equilibrium between the break liquid and atmosphere. Consequently, Equation (104) is used to calculate the evaporation (or flashing) flow rate. The results are presented in the first row of Table 7-2.

Since the break flow rate drops to essentially zero during the refill time phase, the break pool evaporation rate during refill is assumed to be zero.

The break pool surface area changes with time as the pool level rises. Since the analysis shows the evaporation rate is a small fraction of the flow into the pool, the pool liquid volume can be estimated as the integral of the flow rate over time. Using the liquid flow rates and times of each phase from Table 6-3, the pool volume at the start of each time phase was calculated and the pool surface area was determined from the relationship between break pool volume and surface area shown in Figure 3-8. The results are summarized in Table 7-3.

Inspection of the detailed energy pi groups in Table 8-4 shows that during all the phases of a DECLG LOCA, phenomena associated with the drops, pools, chimney, and baffle are not important and can therefore be neglected since the pi group numerical values are of order less than 0.1. The only pi groups of any significance are those associated with the solid internal heat sinks and the shell. However, the internal heat sinks become saturated prior to the time when quasi-steady operation occurs. Therefore, only the pi groups identified as containment or shell were calculated for the AP600 plant and the LST, at steady-state.

The results of the energy scaling comparison between the LST and AP600 are summarized in Table 10-3. The transient pi group $\pi_{e,\tau}$ is not applicable since $d(\mu)^*/dt^* = 0$, that is, the containment atmosphere is in a quasi steady-state condition. Since the pi groups are normalized on break energy, $\pi_{e,brk} = 1.0$. The table shows the dominant phenomena are condensation on the inside of the shell, $\pi_{e,fg,ns}$, and evaporation on the exterior of the shell, $\pi_{e,fg,esx}$. The values for $\pi_{e,fg,ns}$ and $\pi_{e,fg,esx}$ in Table 10-3 show the dominant phenomena (condensation and evaporation) compare favorably. The shell energy phenomena for the subcooled and dry shell, $\pi_{e,q,ns}$ and $\pi_{e,q,ssx}$ are shown to be second-order phenomena. Although the pi values for subcooled and dry energy do not compare quite as well as those for condensation and evaporation, the former are second-order phenomena in both the plant and test, so distortions are not significant.

The scaling comparison permits the conclusion that the scaled LST represents the dominant internal and external phenomena in AP600 with sufficient accuracy that the tests can be used to validate computer codes during quasi-steady (long-term) operation.

10.2.3 Scaling of the Transition Between the Initial Transient Phase and Quasi-Steady Phase

There is no single LST experiment that is well-scaled over the entire range of the AP600 DECLG LOCA. However, there is a wide range of LST experimental data that can cover the transient in a piece-wise fashion. The previous sections (10.2.1 and 10.2.2), for example, used different test runs to demonstrate that the LST adequately scales the initial transient range and long-term portions of the DECLG LOCA transient from a global, system level, for code validation purposes.

Test data at intermediate thermodynamic conditions (from the other test runs) could be used, applying the same scaling equations developed in Section 10.2.1 to confirm scaling in the transition between the initial transient phase and the quasi-steady phase. However, this is not necessary since the system level scaling has already been shown to be adequate in both the initial and long-term phases which bound the overall range of the transient.

Thus, it can be concluded that the use of the matrix of LST tests is sufficient for determining the effect of WGOTHIC lumped parameter biases in application to AP600.

ATTACHMENT 3

Markups to WCAP-14812 Rev 1, "Accident Specification and Phenomena Evaluation for AP600 Passive Containment Cooling System"

The following comments consider Westinghouse response to discussion items that were raised concerning WCAP-14811, Rev. 0, the earlier version of the PIRT report, and how these are addressed in WCAP-14812, Rev. 1.

1. Time phases in Table 4-1 are not consistent with the scaling report, WCAP-14845, Rev. 2 (Table 6-3).

RESPONSE:

The time phase difference results from the selection of different times for the peak pressure in the PIRT and in the scaling analysis. The time for the PIRT peak pressure was defined from the SSAR LOCA transient. The time for the scaling analysis peak pressure was selected for a fictitious transient that produced a peak pressure equal to the design pressure. The latter case produced an upper limit for the scaling analysis.

- (2.) There still seems to be inconsistencies in the ranking of phenomena between the PIRT and scaling reports. For example, break source item 1E droplet/liquid flashing is rated low for all accident phases but still appears in the list of medium and high ranked phenomena in Table 2-1 of the scaling report.

RESPONSE:

The PIRT is the source document for ranking. The scaling analysis WCAP-14845, Table 2-1 will be revised to delete items from the column labeled "phenomenon" that are ranked Low for all phases of LOCA and MSLB. The items to be deleted are: 1E) droplet/liquid flashing, 3A) Liquid Film Energy Transport, 5F) Break Pool Compartment Filling (flooding level), 7A) Convection from Containment, and 7B) Radiation from Containment.

3. In Appendix A, Westinghouse has now at least identified the experts by name, but still hasn't identified opinions and positions with an expert, so that the reader cannot tell who held what opinion. Also, source documents, such as written materials from the experts, are not included. The value of the expert judgments is reduced considerably by the lack of information in this area.

RESPONSE:

Westinghouse has considered the comments of the NRC, the ACRS, and the experts on source identification and believes the PIRT embodies the best balance. Source documents related to the expert review are available for NRC review at Westinghouse.

- (4.) Pg. 2-3: The following sentence is unclear:

Such active systems in current PWRs lead to somewhat different thermal hydraulic conditions in AP600, so that AP600 specific verification was needed.

Suggest rephrasing the sentence with something like:

The absence of such active systems lead to somewhat...

RESPONSE:

The text in WCAP-14812 will be revised to clarify the sentence.

5. Pg. 2-3/2-4: Scaling has been used to confirm the PIRT ranking (Ref. 2, Section II) and to specify the applicable data from the PCS Large Scale Test (Ref. 2, Section III) for separate effects correlation validation and WGOTHIC code validation.

The same test data may have been used for both:

- a) deriving bounding correlations and
- b) for WGOTHIC code validation.

Multiple uses of the same data source may lead to circular arguments. Please discuss the procedures Westinghouse used to maintained the integrity of the validation studies.

RESPONSE:

The same test can be used for both without introducing circular logic. For example, correlations for the mass transfer rate and for water coverage were determined from the LST data and validated without use of the code. The models were built into, or input to the code, and it was verified that the code gave the same mass transfer rate and coverage predictions. This is not circular. The code was then used to predict pressure in the LST and compared to measurements. Since the individual models and the pressure calculations use independent data, the logic is not circular.

6. Pg. 2-4: Westinghouse states that the integral LST facility included a representation of the AP600 internals. Although the LST internals did not represent inter-compartment flow paths, data from LST have been considered in addressing stratification since the LST test matrix addressed a range of imposed boundary conditions. Does this limit the LST data applicability to stratification only?

RESPONSE:

No, it limits the LST to use as separate effects test data and as integral effects that do not include similarity of internal circulation.

(7.) Pg. 2-9: Section 2.2.7 LST, States:

Long-term heat and mass transfer test data for a geometrically similar model of the AP600 containment vessel..... determining the relative importance of various parameter that affect heat and mass transfer on both inside/outside containment surfaces.

What does relative importance means? What is the measure?

RESPONSE:

The sentence will be revised something like " ... for determining the sensitivity of the heat and mass transfer rates inside and outside containment to various parameters."

(8.) Pg. 2-11: In the LST, a diffuser was located under a simulated steam generator compartment below operating deck (LOCA simulated). Steam rose in a plume, and air was entrained in the rising plume resulting in a natural circulation flow pattern within the simulated containment.

However, a diffuser under a simulated SG-compartment in LST does not provide anything close to real break simulation (LOCA blowdown). How can a plume develop for an unconfined SG? LST lacks a second SG-compartment, therefore flows and entrainment are atypical of AP600.

RESPONSE:

The paragraph that precedes the subject paragraph states "The LST did not simulate the blowdown phase of the LOCA or MSLB transients." The text in the subject paragraph will be revised to state that the diffuser simulated the break location of a LOCA.

Pg. 2-11 : Section 2.3 : Scaling Analysis

(9.) Last paragraph, Westinghouse states :

In Reference 2, Sect. III, top-down scaling is used to determine the most important system level phenomena during blowdown and long-term phases of a large break LOCA transient and to show how well those phenomena are preserved between LST and the AP600 plant. The results of this analysis are used to determine to what extent global containment data (pressure) can be used from LST for WGOETHIC code validation. This contradicts the statements in Section 2.2.7 stating the LST did not simulate the blowdown phase.

RESPONSE:

Section 2.2.7 of WCAP-14812, Rev. 1 (3rd paragraph) will be revised. The sentence, "The LST did not simulate the blowdown phase of the LOCA and MSLB transients." will be deleted. The last sentence of the paragraph will be revised to read, "LST tests were performed over a range of initial and boundary conditions to assess the impact on heat and mass transfer rates, and to provide a sufficient history of thermodynamic conditions to adequately simulate the quasi-steady long term cooling phase of an AP600 transient."

The last paragraph of WCAP-14845, Rev. 2, Section 10.2.1.3 provides further clarification of the use of LST data during the blowdown phase of the transient.

10. The break source definition (For what break? LOCA? MSLB?) is not detailed enough as it only relates to the blowdown phase. The water drops suspended in the steam initially flash a small fraction of their mass to steam to reach thermal equilibrium within the containment atmosphere.

RESPONSE:

Sections 3.2.1, 3.2.2, and 3.2.3 are brief, general descriptions of the two major regions (inside and outside) that are separated by the shell. It is not intended to be detailed, but rather, to encompass both LOCA and MSLB transients. The details of the Evaluation Model are presented in WCAP-14407, Rev. 1, Section 4.

11. After flashing, the large surface area of these many tiny water drops maintains the atmosphere at or near saturation for up to thousands of seconds. Westinghouse needs to provide references and experimental evidence.

RESPONSE:

The scenario in question was postulated as an extreme (drops may very well not persist for more than a few 10's of seconds) that is analyzed to determine how significant an effect drops can have, both drop thermal and momentum effects. The outcome of the analysis is that both effects are ranked low for all time phases. Therefore, the effects of real drops are no more important than these hypothetical drops.

12. All compartments below-deck are provided with top openings to minimize the potential for a dead pocket of noncondensable concentration. However, this is not applicable for higher up break positions for steel jacketed concrete (explanation missing). The break liquid which is not dispersed as drops is assumed to leave the break at the containment saturation pressure.

RESPONSE:

Break liquid not dispersed as drops is addressed in Section 4.4.1E (PIRT).

The geometry of the internal heat sinks above the operating deck is also designed to minimize the potential for dead pockets of noncondensibles.

Additional agenda items:

Ref.: Loftus, M.; Spencer, D.; Woodcock, J., "Accident Specification and Phenomena Evaluation for AP600 Passive Containment Cooling System," WCAP-14812, Rev. 1, June 1997

The following general observations, issues and comments are provided concerning WCAP-14812, Rev. 1:

- 1) The current PIRT-report is not code-independent but rather merges PIRTs, WGOthic Evaluation Model aspects and uncertainty issues in one and the same document. This should be reflected in the title of the report.

COMMENT:

THE COMMENT IS NOTED AND ACKNOWLEDGED THAT BOTH WGOthic, ASPECTS OF THE EVALUATION MODEL AND CERTAIN ELEMENTS OF UNCERTAINTY ISSUES ARE DISCUSSED IN THE CURRENT PIRT REPORT. THE PRIMARY FOCUS OF THE CURRENT PIRT DOCUMENT IS TO PRESENT AND DISCUSS THE PIRT. IT IS NOTED THAT WGOthic, THE EVALUATION MODEL AND UNCERTAINTY ISSUES ARE DISCUSSED TO THE EXTENT THEY SUPPORT DEVELOPMENT AND UNDERSTANDING OF THE PIRT. THUS, THE TITLE OF THE DOCUMENT IS INDICATIVE OF ITS CONTENT AND NO CHANGE IN THE TITLE OF THE CURRENT PIRT REPORT IS PLANNED.

- (2.) The ranking rationale as displayed on pg. 4-20 deviates from PIRT guidelines as it lists both energy transfer process and containment pressure. The chosen wording opens many avenues for ambiguity and speculation. If it is decided to really keep two objective functions, namely "energy transfer process" and "containment pressure reduction" then the items in the ranking rationale should correctly read "increase in energy transfer" and resultant "containment pressure reduction." This could be also reconciled by eliminating the word "reduction."

COMMENT:

CONTAINMENT PRESSURE WAS THE PREFERRED FIGURE OF MERIT USED FOR THE PIRT. HOWEVER, CONTAINMENT PRESSURE IS MEANINGFUL ONLY FOR PARAMETERS DEFINED INSIDE THE CONTAINMENT SHELL. FOR PARAMETERS CONSIDERED EXTERNAL TO THE CONTAINMENT SHELL, THE ENERGY TRANSFER PROCESS WAS USED AS THE FIGURE OF MERIT. THE TEXT WILL BE AMENDED TO CLARIFY THIS.

- 3) Although the ranking rationale encompasses both energy transfer process and containment pressure, the texts, references and arguments for the individual phenomenon in the main body of the report refers to the containment pressure only for the majority of them because this is the only figure of merit for which results have been provided.

COMMENT:

CONTAINMENT PRESSURE WAS THE PREFERRED FIGURE OF MERIT USED FOR THE PIRT. HOWEVER, CONTAINMENT PRESSURE IS MEANINGFUL FOR PARAMETERS DEFINED INSIDE THE CONTAINMENT SHELL. FOR PARAMETERS CONSIDERED EXTERNAL TO THE CONTAINMENT SHELL, THE ENERGY TRANSFER PROCESS WAS USED AS THE FIGURE OF MERIT.

- 4) Westinghouse has applied the bounding methodology for High-ranked phenomena, such as for instance for the most important energy transfer processes: condensation and evaporation inside and outside the containment, respectively, rather than as recommended for the Low-ranked phenomena.

COMMENT:

THE APPROACH TAKEN BY WESTINGHOUSE TREATS LOW-RANKED PHENOMENA IN A CONSERVATIVE MANNER. NO CHANGE TO THIS CONSERVATIVE TREATMENT OF LOW-RANKED PHENOMENA IS PLANNED.

- 5) The basis for PIRT ranking is not based on experimental evidence (even for High-ranked phenomena) as would be expected. Rather, the majority of PIRT-ranking is based on scaling calculations, done using a special code with a simple model of the containment.

COMMENT:

AS DESCRIBED IN THE DOCUMENT, THE BASIS FOR THE PIRT IS HISTORICAL EXPERIMENTAL DATA WHERE AVAILABLE, HISTORICAL CALCULATIONS, AND EXPERT OPINION. THE DATA, ANALYSES AND EXPERT OPINION USED TO DEVELOP THE PIRT ARE DESCRIBED UNDER THE TITLE, "BASIS FOR PIRT RANKING," GIVEN FOR EACH PHENOMENA LISTED IN THE PIRT. BRIEF DESCRIPTIONS OF TESTS USED FOR DEVELOPMENT OF THE PIRT ARE GIVEN IN SECTION 4.3 OF THE DOCUMENT. EXPERT OPINION USED IN DEVELOPMENT OF THE PIRT IS GIVEN IN APPENDIX A OF THE DOCUMENT. OPTIMAL USE OF AVAILABLE EXPERIMENTAL DATA WAS MADE IN DEVELOPING THE PIRT.

- (6.) Although the majority of PIRT-rankings is based on the results of scaling considerations and expert review, Westinghouse did not specify criteria for the numerical values for the PI-ratios for which the importance of a phenomenon would be ranked differently although they have essentially the same values for the PI-ratios. This leads to a non-uniform ranking, rationale and resultant confusion.

COMMENT:

SEE ATTACHED RESPONSE.

- 7) Westinghouse has evaluated the PI-ratios at the beginning of a time phase. Some physical quantities drastically change over the time phase but this change was not evaluated. Therefore, the numerical FI-ratio evaluated at the beginning of the next time phase, for instance, refill, results in a very much different (higher) value. In some cases, Westinghouse noticed and commented on these discrepancies. However for the majority of phenomenon the low predicted PI-ratios were taken at face value and the phenomenon ranked "Low" for this time phase without any further considerations. This uneven approach leads to a number of ambiguities and concerns.

COMMENT:

IF A PI-GROUP WAS RATED EITHER "HIGH" OF "MEDIUM" FOR ANY PHASE OF THE TRANSIENT, IT WAS TREATED AS A "HIGH" OR "MEDIUM" FOR THE ENTIRE TRANSIENT WITH RESPECT TO TREATMENT IN THE EVALUATION MODEL.

- 8) Most subsections in the discussions on phenomena are geared too much toward the LOCA time phase, although MSLB results in the highest computed containment pressure by the AP600 EM. In most descriptions, MSLB is not mentioned at all except for the PIRT-ranking. This may be acceptable for equally ranked phenomena, but for all other cases this may pose the potential for omitting important information. The non-uniform treatment of LOCA and MSLB time phases does not seem justified.

COMMENT:

THE CONTAINMENT RESPONSE TO A LOCA IS MORE COMPLEX THAN THAT FOR A POSTULATED MSLB. THE APPARENT FOCUS OF ATTENTION ON A LOCA IS THE RESULT OF ACCOUNTING FOR THE INCREASED COMPLEXITY OF THE CONTAINMENT RESPONSE TO A LOCA. WHEN MSLB HAS A UNIQUE ASPECT, IT IS DISCUSSED.

- 9) Some high-ranked phenomena, such as evaporation of the external liquid film, require the success of a medium- and low-ranked phenomenon, i.e., PCS riser annulus natural circulation, vapor acceleration, fog and flow stability. Based on this PIRT, modelers may mistakenly downgrade the conservatism of models associated with critical systems.

COMMENT:

RANKING A PHENOMENA AS "LOW" INDICATES THAT THE PHENOMENA HAS A SMALL EFFECT ON PRESSURE. IT COULD BE TREATED WITH REALISTIC OR BEST ESTIMATE MODELS, OR IGNORED IF SUCH TREATMENT WOULD BE CONSERVATIVE. SIMILARLY, PHENOMENA RANKED AS A "MEDIUM" AT ANY TIME DURING THE TRANSIENT WERE SPECIFICALLY CONSIDERED DURING IN THE EVALUATION MODEL AND WOULD BE IGNORED ONLY IF TO DO SO WOULD BE CONSERVATIVE (RESULT IN A PRESSURE INCREASE). THUS, THE CONSERVATISM ASSOCIATED WITH TREATMENT OF PHENOMENA RANKED AS "HIGH" WAS NOT CHALLENGED BY EITHER "MEDIUM" OR "LOW" RANKED PHENOMENA.

- 10) Westinghouse may not be crediting the expert review efforts, because of the following reasons:
- a) The expert review is no substitute for an independent PIRT panel.
 - b) There is not a single phenomenon for which Westinghouse has adopted the experts' different ranking. Rather the experts' opinions were dismissed and the results of the scaling PI-ratios were adopted (compare comment under point) maintaining Westinghouse's original ranking. Most often the experts ranked the phenomenon higher but Westinghouse consistently downgraded the rank.

This is acceptable only for phenomena for which an in-depth knowledge and experimental database exists. Most often this is not the case in the ranking should tend toward higher than lower importance.

COMMENT:

WHERE THE PIRT RANKING DEVELOPED BY WESTINGHOUSE DIFFERED FROM THAT OF EXPERT REVIEW, JUSTIFICATION FOR THE DIFFERENCE WAS GIVEN. THE REVIEW OF DIFFERING OPINIONS AND DEVELOPMENT OF RATIONALE ACCEPTING OR REJECTING EXPERT REVIEW IS ALSO PART OF THE PIRT PROCESS. IT IS WESTINGHOUSE'S OPINION THAT THE JUSTIFICATION DEVELOPED FOR VARYING FROM THE EXPERT REVIEW RANKING AND PRESENTED IN REVISION 1 OF WCAP-14812 IS TECHNICALLY VALID.

- 11) Descriptions under the headline "How Phenomenon is Implemented in Evaluation Model" do not actually refer to the implementation but rather to input quantities or general descriptions of the phenomenon/process in or between components/subsystems. In fact, for many phenomena the text is a repeat of at least parts of the general introductory description of the phenomenon under consideration. Under the headline one would expect reference to models, correlations/procedures implemented in WGOthic.

COMMENT:

THE DESCRIPTIONS ARE GENERALLY SUMMARY STATEMENTS. HOWEVER, WHERE THE DETAILS MAY BE FOUND ARE INCLUDED BY REFERENCE. INCLUSION OF ALL DETAILS IN THIS REPORT WOULD HAVE BEEN REPETITIOUS AND MADE THE REPORT UNWIELDY AND DIFFICULT TO USE. DETAILS OF THE IMPLEMENTATION IN WGOthic IS FOUND IN WCAP-14407.

- 12) Westinghouse lists a number of "Test Experience" under the headline "Justification for EM Treatment of Phenomenon." However, for many phenomena this consists only of a test description or reference of a correlation which is not really a justification. Under justification it would be expected to reference results how the containment pressure/energy transfer processes are affected using the cited correlation in comparison with data. This has not been done consistently, rather sensitivity studies and LST-result comparisons are references. In hindsight, the test experience cited should well have been referenced as basis for the PIRT-ranking (compare comment under point) rather than for justification of WGOthic AP600 EM.

COMMENT:

THE INFORMATION SUGGESTED IN THIS COMMENT IS INCLUDED BY REFERENCE. INCLUSION OF THE DETAILS IN THIS REPORT WOULD HAVE BEEN REPETITIOUS AND RESULTED IN AN UNWIELDY REPORT.

Issues Related to the Ranking of Specific Phenomena and Treatment in EM

General comment: The phenomena listed under the components are not systematically handled in terms of time phases in Section 4.1.

Pg. 4-8 Table 4-1

- 1) Westinghouse ranks all characteristics (direction, elevation, momentum, density) of (1) Break Source "Low" during LOCA long-term. Equally, inter-compartment flow for (2) Containment volume is ranked "Low" for LOCA blowdown phase and so on. Given the fact that LST did not consistently cover all these phenomena with respect to AP600 requirements, the ranking seems too low especially when considering the impact of "memory effect" of early heatup in one region of the plant on global natural circulation pattern during the LOCA long-term time phase. This concern also encompasses the inter-compartment flows as this determines the region of initial heatup.

COMMENT:

THE BASIS FOR THE RANKING OF BREAK SOURCE PHENOMENA AS BEING "LOW" DURING THE LONG TERM LOCA IS BASED ON KNOWING THAT MASS AND ENERGY RELEASES ARE SMALL DURING THIS TIME PERIOD, NOT ON TEST DATA. SIMILARLY, FOR INTER-COMPARTMENTAL FLOW, THE "LOW" RANKING IS BASED ON SENSITIVITY STUDIES WHICH SHOW THE DETAILS OF THE FLOW PATHS ARE NOT IMPORTANT.

- 2) The component/subsystem (5) Break pool does not list pool heatup as a phenomena. Is there any special consideration why Westinghouse has disregard this potential source for energy release during long-term?

COMMENT:

DURING THE LONG TERM, THE BREAK POOL FLOODS UP TO ABOVE THE BREAK LOCATION. HEAT-UP OF THE BREAK POOL IS BY CONDENSATION OF STEAM ON THE SURFACE OF THE BREAK POOL. SINCE, LONG TERM, THE BREAK POOL IS RELATIVELY QUIESCENT (LOW FLOW OUT THE BREAK), THE CONDENSATION PROCESS IS LIMITED BY THE FORMATION OF A WARM LAYER OF FLUID ON THE TOP OF THE BREAK POOL. THUS, THE HEATUP OF THE BREAK POOL IS LIMITED.

- 3) Under point (7) Steel Shell and energy transport phenomena have been ranked either "Low" or "Medium", yet the energy removal from the film evaporation (ranked High) is mandatory in order to guarantee the efficiency of the passive PCS cooling. Westinghouse is asked to provide information about the ranking rationale applied for energy transport phenomena in the downcomer riser component.

COMMENT:

THE PRIMARY COOLING MECHANISM FOR THE AP600 CONTAINMENT IS BY EVAPORATION OF THE PCS FLOW. THUS, AS LONG AS WATER IS APPLIED TO THE EXTERNAL SURFACE OF THE PCS SHELL, IT IS EXPECTED THAT THERMAL ENERGY TRANSPORT MECHANISMS OTHER THAN EVAPORATION WOULD BE RANKED AS EITHER MEDIUM OR LOW. OF COURSE, IF THE SHELL WERE INSULATED, THEN THERE WOULD BE NO ENERGY TRANSFER. HOWEVER, THE PURPOSE OF THE RANKING IS TO MAKE JUDGEMENTS REGARDING THE IMPACT OF UNCERTAINTIES ASSOCIATED WITH INDIVIDUAL ENERGY TRANSPORT PROCESSES. THUS, IN RANKING THE CONDUCTION THROUGH THE STEEL SHELL, NOTING THAT IT REPRESENTS ONLY ABOUT 1/3 OF THE TOTAL RESISTANCE AND THAT SHELL THICKNESS IS WELL CONTROLLED, THE EXPERTS AGREED THAT CONDUCTION THROUGH THE SHELL SHOULD BE RANKED OF LOWER IMPORTANCE THAN CONDENSATION OR EVAPORATION.

- 4) Under point (8) PCS Cooling Water, subpoint D) Film Striping received only "Low" ranks for all time phases, yet this is the cause for introducing a correction for accounting for 2-D heat conduction effects to increase film evaporation. Westinghouse is asked to explain the "Low" ranking for this phenomena even for later phases when film flow is low.

COMMENT:

THIS SECTION IS "STRIPPING," WHICH REFERS TO THE DETACHMENT OF THE LIQUID FILM FROM THE EXTERNAL SURFACE OF THE SHELL DUE TO SHEAR FORCES FROM THE PCS AIR FLOW, AND NOT "STRIPING," WHICH REFERS TO THE FORMATION OF ALTERNATING WET AND DRY STRIPES OF WATER AS IT FLOWS DOWN THE OUTSIDE OF THE CONTAINMENT SHELL. THE "STRIPPING" PHENOMENA IS APPROPRIATELY RANKED AS BEING "LOW."

- 5) Under point (10) Baffle, subpoint G) potential leaks through the baffle are ranked "Medium" for LOCA time phases peak pressure and long-term. Westinghouse is asked to explain this ranking in view of the fact that this poses a potential threat for short-circuiting and thereby disabling the natural draft effect.

COMMENT:

THE RANKING ACKNOWLEDGES THE POTENTIAL IMPORTANCE OF BAFFLE LEAKAGE. THE INTRODUCTORY TEXT ALSO NOTES THAT EXPERIMENTAL DATA FOR RECTANGULAR CROSS-SECTION CHANNELS SHOWS BAFFLES HAVING LIMITED EFFECT ON HEAT TRANSFER. WHILE NOT EVALUATED AS BEING A DOMINATE PHENOMENA, THE RANKING OF "MEDIUM" ASSURES THE PHENOMENA IS ADDRESSED IN THE AP600 CONTAINMENT EVALUATION MODEL.

SHORT-CIRCUITING HAS BEEN EVALUATED WITH SENSITIVITIES AND SHOWN TO BE A MEDIUM EFFECT. NOTE ALSO THAT THE EVALUATION MODEL INCLUDES A FLOW PATH ACROSS THE BAFFLE TO ACCOUNT FOR THE POTENTIAL FOR LEAKAGE.

- 6) Under point 13) Downcomer, subpoints A) PCS Natural Circulation and B) Air Flow Stability are ranked "Medium" and "Low", respectively, yet the efficiency of the PCS system depend very much on sustaining both phenomena, for transport purposes of the evaporation mass and energy from the cooling film. Westinghouse is asked to provide the ranking rationale for both phenomena given their importance for the functionality of the PCS cooling concept.

COMMENT:

FOR PCS NATURAL CIRCULATION, THE RANKING OF MEDIUM WAS BASED ON STUDIES SHOWING THE SENSITIVITY OF THE PCS AIR FLOW TO HYDRAULIC PARAMETERS WAS SMALL.

FOR AIR FLOW STABILITY, THE RANKING OF LOW WAS BASED ON SCALING THE ENERGY AND MOMENTUM ASSOCIATED WITH THE FLOW PATH. THE STUDY SHOWED THAT ENERGY ADDITION TO THE DOWNCOMER FROM THE BAFFLE WAS SMALL AND THE MOMENTUM OF A BUOYANT BOUNDARY LAYER WOULD NOT DISRUPT THE ESTABLISHED NATURAL CIRCULATION FLOW. THUS THE POTENTIAL FOR INSTABILITY TO OCCUR IN THE PCS AIR FLOW PATH IS NEGLIGIBLE, AND THE PHENOMENON IS THEREFORE RANKED LOW.

Westinghouse states that increased heat transfer coefficients were observed when the steam jet directly impinges on the horizontal plate and that this simulates the steamline break. Westinghouse is asked to provide information why this is the case, given the fact that the realistic break positions for both LOCA and MSLB are still not displayed in the associated figures.

COMMENT:

THE SUBJECT FIGURE 3-2 CLEARLY SHOWS THE PRIMARY SYSTEM PIPE WHICH GOES FROM THE STEAM GENERATOR TO THE REACTOR VESSEL AT THE BOTTOM OF THE STEAM GENERATOR COMPARTMENT, AND THE MAIN STEAM LINE WHICH LEAVES THE TOP OF THE STEAM GENERATOR AND PASSES THROUGH THE CMT COMPARTMENT BEFORE IT PENETRATES THE CONTAINMENT SHELL. IF THE READER IS INTERESTED IN MORE DETAIL, HE IS REFERRED TO WCAP-14407, FIGURE 9-36, WHICH SHOWS IN MORE DETAIL THE ARRANGEMENT AND VARIOUS DIRECTIONS AND MOMENTUM EFFECTS EVALUATED IN ESTABLISHING THE LIMITING LOCA AND MSLB SCENARIOS. THE STATEMENT REFERS TO OBSERVED BEHAVIOR IN EXPERIMENTS. THE TEST WAS DESIGNED TO SIMULATE CONDITIONS EXPECTED FROM A STEAM LINE BREAK THAT WOULD RESULT IN STEAM IMPINGING DIRECTLY ON THE CONTAINMENT WALL. THE SUBJECT TEXT IS NOT INTENDED TO IMPLY THAT ALL STEAMLINE BREAKS WOULD RESULT IN A STEAM JET IMPINGING ON THE CONTAINMENT SHELL.

Westinghouse reports observations from the Small Scale PCS Integral Tests concerning higher than vessel-averaged heat removal at the top of the dome. However, the phenomenon of non-uniformity in heat transfer is not listed in the PIRTs. Does this mean that this phenomenon has not been observed during LST-tests?

COMMENT:

IN REVIEWING THE PIRT FORMAT WITH EXPERTS, IT WAS AGREED THAT AN APPROPRIATE LEVEL OF DETAIL WAS INCLUDED IN THE PIRT. THE ADDITION OF ALL PARAMETERS WHICH INFLUENCE EACH PHENOMENON WOULD MAKE THE PIRT UNWIELDY AND REDUCE ITS USEFULNESS. PARAMETERS WHICH INFLUENCE IMPORTANT PHENOMENA ARE EVALUATED IN ESTABLISHING THE RELEVANT ELEMENTS OF THE CONSERVATIVE EVALUATION MODEL. NON-UNIFORMITY OF HEAT FLUX IS ENCOMPASSED BY OTHER PHENOMENA LISTED IN THE PIRT. THE SUPPLEMENTAL INFORMATION REFERENCED IN THE PIRT POINTS THE READER TO THE SUPPLEMENTAL DOCUMENTATION WHERE MORE DETAIL MAY BE FOUND.

NON-UNIFORMITY OF HEAT FLUX IS ADDRESSED IN THE CIRCULATION AND STRATIFICATION SUPPORTING ELEMENTS OF THE EVALUATION MODEL BASED ON INTERNATIONAL TEST DATA THAT INCLUDES VARIOUS EXTERNAL BOUNDARY CONDITIONS WITH AND WITHOUT EXTERNAL WATER (SECTION 9.C.2 OF WCAP-14407). THE INFLUENCE OF AXIALLY VARYING HEAT FLUX ON EXTERNAL WATER COVERAGE IS INCLUDED IN THE SECTION 7 WATER COVERAGE EVALUATION.

- 1) Westinghouse reports film behavior during the LST PCS Integral Tests, yet is unclear what the governing heat fluxes were at the outside steel shell surface and how they compare with the relevant ones for AP600.

COMMENT:

ADDITIONAL DISCUSSION IS PROVIDED IN SECTION 7 OF WCAP-14407. ALSO, TABLE 7-5 COMPARES HEAT FLUXES FROM PCS LARGE SCALE TESTS AND TABLE 7-10 LISTS ESTIMATED HEAT FLUXES FOR THE AP600 UNDER VARIOUS CONDITIONS.

- 2) In this context, Westinghouse states that "striped film coverage provided better heat removal than forced quadrant coverage for the same wetted perimeter." Is this statement referring to an experimental setup or to a calculational exercise?

COMMENT:

THIS IS BASED ON COMPARISON OF OBSERVATIONS FROM LARGE SCALE TESTS 207.1, 207.2 AND 207.3 AND 207.4 AS DESCRIBED IN SECTION 2.1.2 AND SUMMARIZED IN TABLE 2-3 OF REPORT PCS-T2R-050, "LARGE-SCALE TEST DATA EVALUATION."

- 3) Westinghouse states that heat removal rate appeared to be more affected by ambient air temperature than by liquid film temperature. Yet, ambient air temperature was ranked "Low." Westinghouse is asked to explain this effect and whether this effect has been observed in all tests.

COMMENT:

THE CONCLUSION REGARDING RELATIVE EFFECTS OF AMBIENT TEMPERATURE AND FILM TEMPERATURE IS DIRECTLY DERIVED FROM LST DATA AS STATED IN THE REFERENCE 38 LST TEST ANALYSIS REPORT. THE RANKING IS AN INDICATION THAT BOTH EFFECTS WERE SMALL, AND THAT AMBIENT AIR TEMPERATURE WAS THE LARGER OF TWO SMALL EFFECTS. AMBIENT AIR TEMPERATURE DETERMINES THE BUOYANCY HEAD THAT CAN BE GENERATED. THIS BEHAVIOR MAY BE NOTED IN ANY TEST WHERE THE VARIABLE IS THE AMBIENT TEMPERATURE.

- 4) Westinghouse reports that also during the LST-test non-uniform heat flux was observed. Why has this phenomenon not be included in the PIRTs? This seems especially important for the horizontal, high-velocity steam jet injection. Please explain.

COMMENT:

IN REVIEWING THE PIRT FORMAT WITH EXPERTS, IT WAS AGREED THAT AN APPROPRIATE LEVEL OF DETAIL WAS INCLUDED IN THE PIRT. THE ADDITION OF ALL PARAMETERS WHICH INFLUENCE EACH PHENOMENON WOULD MAKE THE PIRT UNWIELDY AND REDUCE ITS USEFULNESS. PARAMETERS WHICH INFLUENCE IMPORTANT PHENOMENA ARE EVALUATED IN ESTABLISHING THE RELEVANT ELEMENTS OF THE CONSERVATIVE EVALUATION MODEL. NON-UNIFORMITY OF HEAT FLUX IS ENCOMPASSED BY OTHER PHENOMENA LISTED IN THE PIRT. THE SUPPLEMENTAL INFORMATION REFERENCED IN THE PIRT POINTS THE READER TO THE SUPPLEMENTAL DOCUMENTATION WHERE MORE DETAIL MAY BE FOUND.

NON-UNIFORMITY OF HEAT FLUX IS ADDRESSED IN THE CIRCULATION AND STRATIFICATION SUPPORTING ELEMENTS OF THE EVALUATION MODEL BASED ON INTERNATIONAL TEST DATA THAT INCLUDES VARIOUS EXTERNAL BOUNDARY CONDITIONS WITH AND WITHOUT EXTERNAL WATER (SECTION 9.C.2 OF WCAP-14407). THE INFLUENCE OF AXIALLY VARYING HEAT FLUX ON EXTERNAL WATER COVERAGE IS INCLUDED IN THE SECTION 7 WATER COVERAGE EVALUATION.

- 5) Westinghouse states that by raising the steam injection location, heat removal rate increased as the steam concentration near the containment shell increases. This is true but this positive effect is offset by the reduction in steam concentration at lower levels by stratification. Westinghouse is asked to provide more quantitative results for these observations.

COMMENT:

A DETAILED DISCUSSION ON THE OBSERVATIONS ASSOCIATED WITH THIS BEHAVIOR IS INCLUDED IN SECTION 2.4, "STEAM INJECTION LOCATION AND FLOW RATE," OF PCS-T2R-050, "LARGE-SCALE TEST DATA EVALUATION."

General Remarks

The summary presentation of experimental results has largely improved and is more focused than before. However, most information are of qualitative, descriptive nature, rather than quantitative solid evidence. Overall, the list of findings seems still too short. The findings should be structured such that the results are directly related to the phenomenon under consideration.

COMMENT:

THE DISCUSSION PROVIDED IN THIS REPORT IS A SUMMARY. DETAILS OF EXPERIMENTAL RESULTS USED TO SUPPORT DEVELOPMENT OF THE PIRT ARE INCLUDED BY SPECIFIC REFERENCES TO APPLICABLE REPORTS IN THE DISCUSSIONS.

Pg. 4-19

Outside Containment

Westinghouse states that "the buoyancy and flow resistance in the PCS air flow path are important and have a strong effect on the evaporation rate." However, both buoyancy and flow resistance are not listed as phenomenon/parameter in the PIRT. If it is assumed that both phenomena were considered to be covered by "natural circulation", these phenomena would only be ranked medium, an apparent inconsistency.

COMMENT:

A MEDIUM RANKING FOR NATURAL CIRCULATION IS APPROPRIATE. IT IS IMPORTANT BUT IS SECOND ORDER RELATIVE TO EVAPORATION WHICH IS RANKED HIGH. SENSITIVITIES TO THESE PARAMETERS IS PROVIDED IN WCAP-14407.

Table 2-1 Phenomena Identification and Ranking Table - Summary of High and Medium Ranked Phenomena

Phenomenon *	Effect on Containment	Pi Groups	Where Addressed	
* Break Source Mass and Energy (1A) and Liquid Flooding (1E) and Evaporation (5B)	The only mass and energy source for containment pressurization	$\pi_{p,g,brk,enth}$ $\pi_{p,g,brk,work}$ $\pi_{p,work,d}$ $\pi_{p,work,p}$	Scaling Analysis	
Gas Compliance (2C)	Stores mass and energy in atmosphere, increasing pressure	$\pi_{p,s}$	Scaling Analysis	
Initial Conditions Inside (4A, 4B, 4C)	Temperature, humidity, pressure affect noncondensables and energy storage	None	Initial Conditions Ref. 5, Section 5	
Containment Solid Heat Sinks (3), Pool (5), Drops (1), and Shell (7)	Store energy (and remove mass from atmosphere) reducing pressure	$\pi_{p,i}$ $\pi_{p,work,i}$	Scaling Analysis *	
* Internal Heat Sink Conduction (3D, 5E, 7D) and Heat Capacity (3E, 7E)	Limits conduction heat transfer into heat sinks, shell, or pool, and through shell. Stratification in the break pool can affect the effective heat capacity of the pool.	parameter	Scaling Analysis	
Heat Transfer Through Horizontal Liquid Films	Water and noncondensable layers on upward facing horizontal surfaces limit heat and mass transfer to horizontal heat sinks	parameter	Scaling Analysis	
Condensation Mass Transfer (3F, 7F)	The single first-order transport process that removes mass and energy from the containment gas	$\pi_{p,work,j}$	Scaling Analysis	
* Break Source Direction and Elevation (3G), Momentum (3H), Density (3I) and Droplets (1E)	Direction, elevation, density, and momentum can dominate circulation and affect condensation rate. Existence of droplets in source during blowdown affects the effective source density.	parameter	Circulation and Stratification, Ref. 5, Section 9	
Circulation and Stratification	Intercompartment Flow (Circulation) and stratification can affect the distribution of steam near heat sinks for condensation heat removal. Rising liquid level blocks lower circulation flow path.	parameters		
Intercompartment Flow				
* Break Pool Flooding Level (5F)				
Source Fog (3J)	Affects circulation and stratification via buoyancy	parameter		

Table 2-1 Phenomena Identification and Ranking Table - Summary of High and Medium Ranked Phenomena (cont.)

Phenomenon *	Effect on Containment	Pi Groups	Where Addressed
Evaporation Mass Transfer	The first-order transport process that removes mass and energy from the evaporating external shell	$\pi_{e,fg,esx}$	Scaling Analysis
PCS Natural Circulation	Convective air flow provides convective heat and mass transfer from containment shell.	parameter	Scaling Analysis
Liquid Film Flow Rate, Water Temperature, Film Stability	Affects the upper limit for water coverage on the external shell	parameter	Film Stability, Ref. 5, Section 7
Liquid Film Energy Transport	<i>Inside:</i> Carries 14 percent of condensation energy to the IRWST and break pool. <i>Outside:</i> Absorbs 8 percent of energy rejected by the external shell surface.	$\pi_{e,l,j}$ See note 1 $\pi_{e,q,ssx}$	Scaling Analysis
Convection Heat Transfer	A second order transport process that removes energy from the containment gas, and from the external shell.	$\pi_{p,q,j}$ $\pi_{e,q,esx} + \pi_{e,q,dex}$ Note 2	Scaling Analysis
Radiation Heat Transfer	A second order transport process that removes energy from the containment gas and from the external shell.	$\pi_{p,q,j}$ $\pi_{e,q,esx} + \pi_{e,q,dex}$ Note 2	Scaling Analysis
Baffle Conduction and Baffle Leakage paths	Conduction through the baffle into downcomer volume and leakage paths can influence the external natural circulation flow rates	$\pi_{e,q,b,i}$ $\pi_{e,q,b,x}$ None for leakage	PIRT Sections 4.4.10D and 4.4.10G

* Indicators in parentheses refer to phenomena in the "Phenomena Identification and Ranking According to Effect on Containment Pressure" (Reference 3, Table 4-1).

Note 1. The fraction of the internal condensation energy carried away by the liquid film is defined by the ratio: $\pi_{e,l,j} / (\pi_{e,l,j} + \pi_{e,fg,j})$, for each heat sink j. The fraction of the external shell heat rejection that goes into the subcooled heat capacity of the external liquid is defined by the ratio: $\pi_{e,q,ssx} / (\pi_{e,q,ssx} + \pi_{e,q,esx} + \pi_{e,fg,esx} + \pi_{e,q,dex})$. The pi group values for AP600 are presented in Section 8.

Note 2. Inside containment $\pi_{p,q,j}$ represents the pressure effect of sensible heat transfer. The sensible heat transfer is approximately 1/2 radiation heat transfer and 1/2 convection heat transfer. Outside containment $\pi_{e,q,esx} + \pi_{e,q,dex}$ represents the sum of the dry and evaporating shell sensible heat transfer, that is approximately 1/2 radiation heat transfer and 1/2 convection heat transfer.

2.2 TESTING PROGRAMS

The need for tests to support the AP600 containment design was identified in the late 1980s. At that time, containment phenomena with characteristics that were unique to AP600 were identified and an initial testing program was defined. The following provides an overview of the test program structured to address 10CFR52.47(b)(2)(i)(A), subsections (1) and (3).

The design basis events calculated for the SSAR are used as a starting point to examine the types of data needed to support containment DBA. Each transient type is examined to see how the uniqueness of the AP600 design imposes additional model verification requirements on the safety analysis code, W Gothic, and supporting models. The differences between the existing PWRs and the AP600 are also considered, since the basis for many of the safety analysis criteria and methods is rooted in the bases for the current generation of PWRs.

The phenomena were compared to the available containment test database (Table 2-1) to indicate the need for additional tests for validating analytical models. The important thermal hydraulic phenomena were identified, and the existing verification for the safety analysis codes was assessed against the current verification of the code, as well as the applicability of the data verification for the AP600 design. The assessment indicated which models required additional verification for the AP600 specific geometry or conditions. The assessment also gave an initial indication of which phenomena are of most importance for representing the passive features of the AP600 safety systems. Although many of the phenomena occur in current PWRs, there are no safety grade active containment cooling systems credited for the containment DBA in the AP600. Such active systems in ^{AP600} ~~current PWRs~~ lead to somewhat different thermal hydraulic conditions ^{than} in AP600, so that AP600 specific verification was needed. Test programs were established to address:

The absence of ~~current PWRs~~

- evaporation and condensation mass transfer, including the effects of hydrogen,
- external air cooling of the steel shell,
- internal circulation and stratification,
- external liquid film distribution (stability and coverage),
- effects of wind and turbulence,
- integral tests focused on long term heat and mass transfer data (the LST).

Separate effects tests were performed at various facilities, as discussed below. Because the initial blowdown period for AP600 is not significantly different from that of current operating plants, integral effects tests, focused on the long term cooling for AP600, were identified to examine the integrated heat and mass transfer behavior of the PCS.

Subsequent to the design of the PCS integral test facilities, scaling methods developed in the 1990s have been applied as described in NUREG/CR-5809. Scaling has been used to confirm the PIRT ranking (Reference 2, Section II) and to specify the applicable data from the PCS

2.2.6 Small-Scale PCS Integral Tests

The small-scale tests were designed to provide heat and mass transfer data for both the inside and outside of the test vessel. The test apparatus consisted of a 3-ft. diameter, 24-ft. high, steel pressure vessel that was internally heated by steam. The vessel was surrounded by a clear, plexiglass shield that formed a 15-in. wide annulus for either forced or natural circulation air flow. The tests were performed with varying steam flow rates, water film flow rates and temperatures, and inlet air flow rates, temperatures, and humidity.

Instrumentation was provided to measure internal steam concentrations, external water evaporation rates, exit film temperatures, air velocity and temperature, and humidity. See Reference 14 for more information on small-scale tests.

2.2.7 Large-Scale PCS Integral Tests

The large-scale PCS test (LST) facility was built to provide long term heat and mass transfer test data for a geometrically similar model of the AP600 containment vessel. The tests provided experimental data for evaluating phenomena inside containment, and for determining the ~~relative importance of various parameters that affect~~ heat and mass transfer ^{rates} ~~on both the inside and outside containment surfaces~~ to various parameters. ^{sensitivity of the} *

The LST consisted of a 15-ft. diameter, 20-ft. high pressure vessel that approximated the AP600 containment vessel at approximately 1/8th linear scale. A plexiglass cylinder was installed around the vessel to form the air cooling annulus (also called the riser in this report). Air flows upward through the annulus via natural circulation to cool the vessel. A fan was located at the top of the annular shell to provide the capability to induce higher air velocities than can be achieved during natural circulation alone, so that riser Reynolds numbers in the range of AP600 could be simulated. A liquid film was applied to the outside of the test vessel to provide evaporative cooling. Two rings of J-tubes provided the capability to apply water in a manner similar to the water coverage observed in the water distribution tests. See Figure 2-2 for an overview of this test facility.

Test conditions were selected to provide steady-state heat and mass transfer data over a range of conditions representative of a DBA. These conditions included pressure, steam flowrate, cooling air flowrate, and water coverage. The LST was designed to sufficiently encompass the conditions expected during long term cooling for the most limiting AP600 transients such as a large cold leg LOCA and MSLB. ~~The LST did not simulate the blowdown phase of the LOCA and MSLB transients.~~ ^{LST} ~~Reactor~~ tests were performed over a range of ~~the~~ initial and boundary conditions to assess the impact on heat and mass transfer rates, and provide a sufficient history of thermodynamic conditions to adequately simulate the quasi-steady long term cooling phase of an AP600 transient. *

[REDACTED] the break location^{for}₂₋₁₁

For most tests, steam was injected through a diffuser located under a simulated steam generator compartment below the operating deck which simulated a LOCA. The steam rose as a plume, and air was entrained in the rising plume resulting in a natural circulation flow pattern within the simulated containment. Thermocouples located on the inner and outer surfaces of the vessel were used to determine the temperature and heat flux distributions. Tests were also performed with an elevated steam source to simulate an MSLB, with parametric variations to examine the effect of source direction and momentum. See References 15 and 16 for more information on these tests.

*

the break location for

2.3 SCALING ANALYSES

The scaling analysis results have been used to support quantification of the importance of various phenomena in the containment cooling process (Reference 17). The scaling analysis performed for the AP600 containment was submitted for review and revised to incorporate NRC comments (References 2, 18).

In Reference 2, Section II, control volume equations were developed to describe the rate of change of the containment gas energy and pressure. These equations were coupled by conductances to energy equations for internal heat sinks and to the external PCS through the shell.

Scaling groups (PI groups) were developed by normalizing and nondimensionalizing the conservation equations, using initial and boundary conditions, in a form that shows the important dimensionless parameters in each group. Values were calculated for the PI groups during each time phase to quantify the relative importance of the transport processes and components. The evaluation of the PI groups assumed that the containment steam/air atmosphere was well-mixed. Nondimensional parameters and relevant test data were defined for assessing stratification and internal flow field stability.

The PI groups were evaluated for containment energy and pressurization, conductances to heat sinks and the shell, momentum in the air flow path, and momentum within the containment. The conclusions from the scaling analysis, which support the importance of the phenomena identified in the PIRT, are discussed in subsection 4.3.2.

In Reference 2, Section III, top-down scaling is used to determine the most important system level phenomena during blowdown and long term phases of a Large LOCA transient and to show how well that phenomena are preserved between the LST and AP600 plant. The results of this analysis are used to determine to what extent global containment data (i.e. containment pressure) can be used from the Large Scale Test (LST) for WGothic code validation.

Additional agenda items:

Ref.: Loftus, M.; Spencer, D.; Woodcock, J., "Accident Specification and Phenomena Evaluation for AP600 Passive Containment Cooling System," WCAP-14812, Rev. 1, June 1997

The following general observations, issues and comments are provided concerning WCAP-14812, Rev. 1:

- 2) The ranking rationale as displayed on pg. 4-20 deviates from PIRT guidelines as it lists both energy transfer process and containment pressure. The chosen wording opens many avenues for ambiguity and speculation. If it is decided to really keep two objective functions, namely "energy transfer process" and "containment pressure reduction" then the items in the ranking rationale should correctly read "increase in energy transfer" and resultant "containment pressure reduction." This could be also reconciled by eliminating the word "reduction."

Comment:

To clarify this point, the text of the first paragraph under "Basis for Ranking" will be replaced with the following:

The phenomena relevant to the containment response to a DBA are shown in the PIRT (Table 4-1). The PIRT has been structured into high, medium and low rankings consistent with the discussion in subsection 4.2. Phenomena were ranked based on their effect on containment pressure as deduced from test results, scaling analysis results, sensitivity studies, expert review and engineering judgement.

Containment pressure was the preferred figure of merit used for the PIRT for containment pressure scaling. However, containment pressure is meaningful only for those parameters defined inside the containment shell (The pressure of the ambient atmosphere is unaffected by the energy transfer from the containment shell.) For parameters considered external to the containment shell, the energy transfer process was used as the figure of merit.

- 6) Although the majority of PIRT-rankings is based on the results of scaling considerations and expert review, Westinghouse did not specify criteria for the numerical values for the PI-ratios for which the importance of a phenomenon would be ranked differently although they have essentially the same values for the PI-ratios. This leads to a non-uniform ranking, rationale and resultant confusion.

COMMENT:

The numerical criteria for establishing a ranking for a phenomenon, based on the scaling analysis results, was:

Low	-	0.0 to 0.10
Medium	-	0.11 to 0.20
High	-	> 0.21

There were a small number of phenomena for which scaling results and expert opinion did not agree. The rationale for selecting the ranking for the phenomenon listed in the PIRT, as well as the phenomena to which that rationale was applied, are summarized below:

Scenario 1: Scaling results rank phenomenon as "Low," expert opinion ranks phenomenon higher; phenomena listed as "Low" in PIRT.

Basis: Sensitivity studies performed to study the effect of the phenomenon supported a PIRT ranking of "Low." Numerical results were given greater weight than expert opinion in setting the PIRT ranking to "Low."

The phenomena to which this scenario was applied in determining its PIRT ranking are listed in the table below.

PIRT Table Component or Volume	Phenomenon Title
1(e)	Droplet / Liquid Flashing
3(a)	Liquid Film Energy Transport on Containment Heat Sinks
5(a)	Break Pool Circulation / Stratification
5(b)	Break Pool Condensation / Evaporation
7(a)	Convection Heat Transfer from Containment Volume
7(b)	Radiation Heat Transfer from Containment Volume to Steel Shell
7(e)	Internal Film Energy Transport on Steel Shell
13(a)	PCS Natural Circulation ⁽¹⁾

Notes: (1) The ranking of "Low" for this phenomenon does not indicate that the presence of natural circulation is unimportant to the predicted AP600 containment response. Rather, sensitivity studies indicate there is a small variation in predicted containment pressures over the range of hydraulic resistances considered for natural circulation air flow for the AP600 design. This is primarily due to the self-compensating nature of the buoyancy-

driven flow; higher hydraulic resistance results in lower air flow which results in higher air temperatures which increases the buoyant forces which increases air velocity which increases the air flow rate

Scenario 2: Expert opinion ranks the phenomenon as "Low," scaling results ranks the phenomenon higher; phenomenon listed as "Medium" or "High" in PIRT.

Basis: In the absence of corroborating numerical results (sensitivity calculations), the higher ranking of the experts was assigned to the phenomenon in the PIRT.

The phenomena to which this scenario was applied in determining their PIRT ranking are listed in the table below.

PIRT Table Component or Volume	Phenomenon Title
3(g)	Convection from Containment Volume
3(h)	Radiation from Containment Volume to Containment Heat Sinks

Scenario 3: This scenario was applicable to these phenomena transferring energy from the containment atmosphere to and through the containment shell; condensation on the inside surface of the shell, heat capacitance of the shell, and thermal conductivity through the shell. In comparing the ranking obtained from expert opinion and scaling calculations, the highest ranking was selected for the PIRT. If the ranking obtained from expert opinion and scaling calculations agreed, that ranking was entered into the PIRT.

Basis: The success of the PCS is dependent upon transferring energy from the containment atmosphere through the containment shell to the ambient environment. Conservatively ranking the importance of those phenomena assures they will be appropriately addressed in the AP600 containment Evaluation Model.

The phenomena to which this scenario was applied in determining its PIRT ranking are listed in the table below.

PIRT Table Component or Volume	Phenomenon Title
7(c)	Condensation on Inside Containment Shell
7(f)	Conduction Through Shell
7(g)	Heat Capacity of Shell

It is also noted that all phenomena ranked as "medium" or "high" in at least one phase of the transient were treated in the same manner for the entire transient. That is, those phenomena were explicitly included in the AP600 containment evaluation model.



Westinghouse
Electric Corporation

Energy Systems

Box 355
Pittsburgh Pennsylvania 15230-0355

DCP/NRC1413
NSD-NRC-98-5757
Docket No.: 52-003

August 14, 1998

Document Control Desk
U. S. Nuclear Regulatory Commission
Washington, DC 20555

ATTENTION: T. R. Quay

SUBJECT: RESPONSE TO NRC LETTERS CONCERNING REQUEST FOR WITHHOLDING
INFORMATION

- Reference:
1. Letter, Sebrosky to McIntyre, "Request for withholding information from public disclosure for Westinghouse AP600 design letter of October 20, 1993," dated June 18, 1998.
 2. Letter, Sebrosky to McIntyre, "Request for withholding information from public disclosure for Westinghouse AP600 design letter of January 17, 1994," dated June 18, 1998.
 3. Letter, Sebrosky to McIntyre, "Request for withholding information from public disclosure for Westinghouse AP600 letters of September 20, 1993, January 21, 1994, and February 3, 1994," dated July 10, 1998.
 4. Letter, Sebrosky to McIntyre, "Request for withholding proprietary information for Westinghouse letters dated April 18, 1995," dated July 15, 1998.
 5. Letter, Huffman to McIntyre, "Request for withholding information from public disclosure of Westinghouse report on AP600 function based task analysis," dated July 17, 1998.

Dear Mr. Quay:

Reference 1 provided the NRC assessment of the Westinghouse claim that proprietary information was provided in a letter dated October 20, 1993, that contained the response to a staff request for additional information regarding the AP600 probabilistic risk assessment. The NRC assessment was that the material was similar to material that exists in the current (1998) nonproprietary version of the AP600 probabilistic risk assessment (PRA) report. In addition, the staff indicated the material was used by the staff in the development of the AP600 draft safety evaluation report and therefore should remain on the docket. At the time this request for additional information response was provided to the

3790a.vpf

~~9808200168~~
APP

ENCLOSURE 2

August 14, 1998

NRC technical staff, the information was considered to be proprietary by Westinghouse since it contained information that had commercial value to Westinghouse. If this request for additional information response was indeed used by the staff in development of the AP600 draft final safety evaluation report in November 30, 1994, then at this time, almost five years later, this information is no longer considered to be proprietary by Westinghouse.

Reference 2 provided the NRC assessment of the Westinghouse claim that proprietary information was provided in a letter dated January 17, 1994, that contained the response to a staff request for additional information regarding the AP600 instrumentation and control system. The NRC assessment was that the material is similar to material that exists in the current (1998) nonproprietary version of the AP600 standard safety analysis report. In addition, the staff indicated the material was used by the staff in the development of the AP600 draft safety evaluation report and therefore should remain on the docket. At the time this request for additional information response was provided to the NRC technical staff, the information was considered to be proprietary by Westinghouse since it contained information that had commercial value to Westinghouse. If this request for additional information response was indeed used by the staff in development of the AP600 draft final safety evaluation report in November 30, 1994, then at this time, over four years later, this information is no longer considered to be proprietary by Westinghouse.

Reference 3 provided the NRC assessment of the Westinghouse claim that proprietary information was provided in a letter dated September 20, 1993, that contained information related to the AP600 PRA and WCAP-13795, which provided the PRA uncertainty analysis. The NRC assessment was that the material was similar to material that exists in the current (1998) nonproprietary version of the AP600 probabilistic risk assessment (PRA) report. In addition, the staff indicated the material was used by the staff in the development of the AP600 draft safety evaluation report and therefore should remain on the docket. At the time this information was provided to the NRC technical staff, it was considered to be proprietary by Westinghouse since it contained information that had commercial value to Westinghouse. If the information transmitted by the Westinghouse September 20, 1993, letter was indeed used by the staff in development of the AP600 draft final safety evaluation report in November 30, 1994, then at this time, almost five years later, this information is no longer considered to be proprietary by Westinghouse.

Reference 3 also provided the NRC assessment of the Westinghouse claim that proprietary information was provided in a letter dated January 21, 1994, that contained WCAP-13913, "Framework for AP600 Severe Accident Management Guidance" (SAMG). The NRC assessment was that the material was similar to material that exists in current (1998) nonproprietary AP600 documents (e.g., WCAP-13914, "Framework for AP600 Severe Accident Management Guidance"). In addition, the staff indicated the material was used by the staff in the development of the AP600 draft safety evaluation report and therefore should remain on the docket. At the time this Framework for SAMG was provided to the NRC technical staff, the information was considered to be proprietary by Westinghouse since it contained information that had commercial value to Westinghouse. At this time, over four years later, this information is no longer considered to be proprietary by Westinghouse.

August 14, 1998

Reference 3 also provided the NRC assessment of the Westinghouse claim that proprietary information was provided in a letter dated February 3, 1994, that contained additional copies of WCAP-13913, "Framework for AP600 Severe Accident Management Guidance" (SAMG). The NRC assessment was that the material was similar to material that exists in current (1998) nonproprietary AP600 documents (e.g., WCAP-13914, "Framework for AP600 Severe Accident Management Guidance"). In addition, the staff indicated the material was used by the staff in the development of the AP600 draft safety evaluation report and therefore should remain on the docket. At the time this Framework for SAMG was provided to the NRC technical staff, the information was considered to be proprietary by Westinghouse since it contained information that had commercial value to Westinghouse. At this time, over four years later, this information is no longer considered to be proprietary by Westinghouse.

Reference 4 provided the NRC assessment of the Westinghouse claim that proprietary information was provided in a letter dated April 18, 1995, that contained information for a MAAP4/RELAP comparison for the AP600 in response to a staff request for additional information. The NRC assessment was that the Westinghouse cover letter indicated that Enclosure 2 is a non-proprietary version of Enclosure 3, however, the staff could not find any portion of the enclosures marked as proprietary. The staff assessment further states the conventional bracketed-superscript notation also appears to be missing. Finally, the NRC assessment states the staff could not determine which part of the material enclosed with the Westinghouse letter was Enclosure 1, 2, or 3. It should be noted that the Westinghouse April 18, 1995, cover letter states "Enclosures 2 (nonproprietary) and 3 (proprietary) provide the requested information." The letter does not indicate that enclosure 2 was a duplicate of enclosure 3 minus the proprietary information. A cover sheet was provided just prior to each of the enclosures to the Westinghouse letter. The enclosures contained the following: Enclosure 1 provided a copy of the NRC's two-page request for information for the MAAP-RELAP comparison. Enclosure 2 provided the requested information, and was titled "Requested Information for AP600 MAAP4/RELAP Comparison." Under section 4, Initial Conditions, of Enclosure 2 it states the initial conditions information (which was proprietary) is provided in Enclosure 3 of the subject Westinghouse letter. Finally, Enclosure 3 contained the list of initial conditions. The information provided in Enclosure 3 was labeled as Westinghouse Proprietary Class 2 at the top of the page, however, the specific proprietary information was not indicated by the bracketed-superscripted notation. In addition to the initial conditions, a mark-up of AP600 PRA Figure K-1 was provided in Enclosure 3. Again, the information was labeled as Westinghouse Proprietary Class 2 at the top of the page, however, the specific proprietary information was not indicated by the bracketed-superscripted notation. At the time the information provided in Enclosure 3 of the subject Westinghouse letter was provided to the NRC technical staff, the information was considered to be proprietary by Westinghouse since it contained information that had commercial value to Westinghouse. At this time, over three years later, this information is no longer considered to be proprietary by Westinghouse.

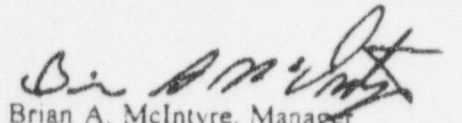
Reference 5 provided the NRC assessment of the Westinghouse claim that proprietary information was provided in a letter dated February 8, 1994, provided a copy of WCAP-13957, "AP600 Reactor Coolant System Mass Inventory: Function Based Risk Analysis." The NRC assessment was that the material was not "information that the staff customarily accepts as proprietary." In addition, the staff indicated the material was used by the staff in the development of the AP600 final safety evaluation report and therefore should remain on the docket. At the time this report was prepared, the

August 14, 1998

information was considered to be proprietary by Westinghouse since it contained information that had commercial value to Westinghouse and was of the type of information that was customarily held in confidence by Westinghouse. That the material was not information that the staff customarily accepts as proprietary is not relevant to making the proprietary determination. However, in an effort to expedite the issuance of the AP600 Final Safety Evaluation Report and Final Design Approval, Westinghouse agrees to no longer consider this information to be proprietary.

In a telephone call on July 8, 1998, the staff informed Westinghouse of a concern related to WCAP-13288 and WCAP-13289, which were associated with the AP600 check valve testing specification. The concern was that the proprietary report had no proprietary information identified and the nonproprietary report had been placed in the public document room. Westinghouse has reviewed these reports and, at this time, considers none of the information to be proprietary.

This response addresses the proprietary issues delineated in the references.


Brian A. McIntyre, Manager
Advanced Plant Safety and Licensing

jml

cc: J. W. Roe - NRC/NRR/DRPM
J. M. Sebrosky - NRC/NRR/DRPM
W. C. Huffman - NRC/NRR/DRPM
H. A. Sepp - Westinghouse